Oxygen diffusion and precipitation in Czochralski silicon

2000 J. Phys.: Condens. Matter 12 R335

(http://iopscience.iop.org/0953-8984/12/25/201)

J. Phys.: Condens. Matter **12** (2000) R335–R365. Printed in the UK PII: S0953-8984(00)73523-5

REVIEW ARTICLE

Oxygen diffusion and precipitation in Czochralski silicon

R C Newman

Centre for Electronic Materials and Devices, The Blackett Laboratory,
The Department of Physics, Imperial College of Science, Technology and Medicine,
London SW7 2BZ, UK

E-mail: r.newman@ic.ac.uk

Received 21 January 2000

Abstract. The objective of this article is to review our understanding of the properties of oxygen impurities in Czochralski silicon that is used to manufacture integrated circuits (ICs). These atoms, present at a concentration of $\sim 10^{18}$ cm^{-3}, occupy bond-centred sites (O_i) in as-grown Si and the jump rate between adjacent sites defines 'normal' diffusion for the temperature range 1325–330 °C. Anneals at high temperatures lead to the formation of amorphous SiO_2 precipitates that act as traps for fast diffusing metallic contaminants, such as Fe and Cu, that may be inadvertently introduced at levels as low as 10^{11} cm^{-3}. Without this 'gettering', there may be severe degradation of fabricated ICs. To accommodate the local volume increase during oxygen precipitation, there is parallel generation of self-interstitials that diffuse away and form lattice defects. High temperature ($T > 700$ °C) anneals are now well understood. Details of lower temperature processes are still a matter of debate: measurements of oxygen diffusion into or out of the Si surface and O_i atom aggregation have implied enhanced diffusion that has variously been attributed to interactions of O_i atoms with lattice vacancies, self-interstitials, metallic elements, carbon, hydrogen impurities etc. There is strong evidence for oxygen–hydrogen interactions at $T < 500$ °C and the formation of fast diffusing O_2 dimers. These observations have led to significant advances in understanding the growth and structures of small oxygen clusters, identified with the so-called thermal donor and shallow thermal donor defects. There is a need to improve this understanding because the temperatures of device processing will continue to decrease as the size of future device features decreases below the lower end of the sub-micron range, currently close to 0.18 μm.

1. Introduction

Single crystals of silicon used for device fabrication are grown either by the floating zone (FZ) or the Czochralski (CZ) technique [1]. The former material is produced by passing a molten zone ($T > 1420$ °C) along the length of a vertical rotating ultra-high purity polycrystalline rod of Si with growth initiated on an oriented seed crystal, usually with a ⟨001⟩ axis. Since neither the solidified parts of the rod nor the molten zone come into contact with other solids, contamination of these crystals is minimized and the high resistivity attainable makes them particularly suitable for the manufacture of high voltage power devices. There are, however, major drawbacks, as explained below, in using these crystals for the fabrication of complex integrated circuits because of the relatively small concentration of incorporated interstitial oxygen impurities ($[O_i] \sim 10^{16}$ cm^{-3}). By comparison, a much higher oxygen concentration of $[O_i] \sim 10^{18}$ cm^{-3} is present in CZ Si that is grown by dipping a rotating seed crystal into molten silicon contained in a silica crucible and then withdrawing the seed slowly. Dissolution of the crucible leads to the melt becoming saturated with oxygen atoms, some fraction of which is subsequently incorporated into the growing crystal with diameters of up to 200 mm and, more recently 300 mm. The O_i atoms are electrically neutral and occupy bond-centred sites

0953-8984/00/250335+31$30.00

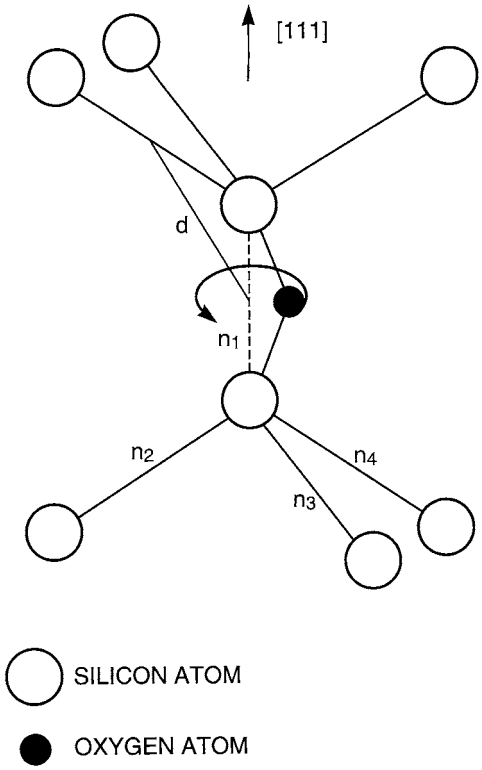

Figure 1. Geometry of a bond-centred interstitial oxygen impurity in silicon showing a small displacement from a ⟨111⟩ axis and the diffusion jump distance d. O_i atoms may be located in any of the four inequivalent bonds and the associated concentrations are designated as n_1–n_4. These concentrations are not all equal when a uni-axial stress is applied to the crystal (see also figure 3).

in the lattice (figure 1), as revealed by high resolution cryogenic Fourier transform infrared (FTIR) absorption measurements (discussed in section 2) [2] and by small increases in the Si lattice parameter, a_0, compared with FZ Si [3].

At room temperature, highly supersaturated CZ Si is stable as the O_i atoms are immobile. During subsequent processing treatments at elevated temperatures, diffusion of O_i atoms leads to their aggregation and the formation of SiO_2 precipitates. Some of these particles grow in the cores of dislocations [4, 5], if they are present, so that glide and dislocation multiplication arising from the build-up of local stresses are inhibited by pinning. Such movement of dislocations, that occurs more readily in FZ Si, leads to the formation of intrinsic point defects (vacancies and self-interstitials) that can lower device yields [6]. SiO_2 precipitate particles, produced at random sites in dislocation-free CZ Si during post-growth anneals, are sinks for fast diffusing Fe, Cu and other metallic atoms [7] that are introduced during device processing. This can occur in spite of the stringent precautions taken to prevent such contamination. The removal of these impurities, especially Fe that reacts with dopant atoms [8] and precipitates as iron silicide causing short circuits [9], is important and can be extremely beneficial: the trapping process is termed intrinsic gettering [10]. In practice, as-grown wafers are first heat treated at a high temperature ($T \sim 1100\,^{\circ}\mathrm{C}$) to cause out-diffusion of O_i atoms, leading to the formation of a so-called 'denuded zone' just below the surface in which the device structure is to be formed. Wafers are then heated at a lower temperature ($T < 750\,^{\circ}\mathrm{C}$) to nucleate small precipitates in the

underlying region and a series of later treatments at higher temperatures, relating to the device fabrication, cause the precipitates to grow [11]. Since FZ Si contains only a small concentration of oxygen there is negligible formation of SiO_2 particles, explaining the advantage of using CZ Si for the manufacture of integrated circuits that involves numerous fabrication steps. It is clearly necessary to control the degree of oxygen precipitation over a wide temperature range.

Understanding the precipitation process would appear to be straightforward since the rate of aggregation of O_i atoms is expected to be controlled by their diffusion coefficient, D_{OXY}, and the driving force for the process should be related to the degree of supersaturation. Accepted values of D_{OXY}, describing 'normal' diffusion, have been obtained from measurements of single atomic jumps at both high and low temperatures, as well as analyses of high temperature in-diffused and out-diffused profiles of ^{18}O or ^{16}O measured by secondary ion mass spectrography (SIMS). These data lead to

$$D_{OXY} = 0.13 \exp(-2.53 \text{ eV}/kT) \text{ cm}^2 \text{ s}^{-1}$$

for the wide temperature range $1325 \geqslant T \geqslant 350\,^{\circ}\text{C}$ (cf the melting point of Si of $1420\,^{\circ}\text{C}$) (figure 2) [12, 13]. If larger values of D_{OXY} are found, the diffusion is said to be enhanced. Some SIMS analyses of diffused profiles generated at high temperatures, but more particularly those in the range 450–650 °C, do reveal enhanced oxygen diffusion that can also occur during aggregation of O_i atoms at lower temperatures. It has been variously proposed that such enhancements are due to interactions of O_i atoms with self-interstitials (I atoms), lattice vacancies (V), a second O_i atom (to form O_2 dimers), fast diffusing metallic contaminants, carbon, nitrogen or hydrogen impurities (section 7). To date, the interactions with hydrogen (or deuterium) impurities, the products of high energy (~2 MeV) electron irradiation (simultaneous generation of I atoms and V) and rapid dimer diffusion appear to be verified by theory and experiment. The enhancement mechanisms are still not fully understood but they are crucially important in relation to controlling the rate of oxygen aggregation at low temperatures ($T < 650\,^{\circ}\text{C}$).

The formation of SiO_2 precipitate particles as a second phase also has its complexity as the ejection of one I atom is required on average to accommodate the local increase in volume [14, 15] for every two O_i atoms that are added to the precipitate. There are therefore two major parallel processes, namely O_i and I-atom diffusion. The latter process leads to the clustering of I atoms and the possibility of I–O_i interactions has to be investigated. In addition, the number density of precipitate particles $n(T)$ formed at a given temperature is increased by the presence of carbon [16], boron [17] or nitrogen [18] atoms: heterogeneous nucleation can then occur as well as homogeneous nucleation. Boron is the standard p-type dopant, carbon impurities are introduced inadvertently during crystal growth, with concentrations that may significantly exceed $\sim 2 \times 10^{15}$ cm^{-3} and nitrogen may be introduced into Si ingots grown from a melt containing silicon nitride (Si_3N_4) [19]. It is clear that $n(T)$ must be determined if the rate of loss of oxygen atoms from solution is to be controlled. At low temperatures ($T < 500\,^{\circ}\text{C}$), the low rate of oxygen diffusion allows the first stage of agglomeration to be attributed to the formation of O_2 dimers [20]. As larger clusters (O_3, O_4 etc) grow, undoped silicon becomes n type due to the formation of donor centres with decreasing ionization energies. These 'thermal donors' have been attributed to the presence of the larger oxygen clusters, as discussed in section 8. In fact, families of these defects form, namely helium-like double thermal donors, TD(N) [21, 22], and three types of single shallow thermal donor [23]. The latter centres incorporate a hydrogen (deuterium) atom, STDH(N), an Al atom, STDAl(N) or another defect X, STDX(N), where X may be a lattice vacancy or a nitrogen atom: $N = 1, 2, 3$ etc is simply a numerical index for successive members of each family. Details of the structures of all four families are still a matter of debate.

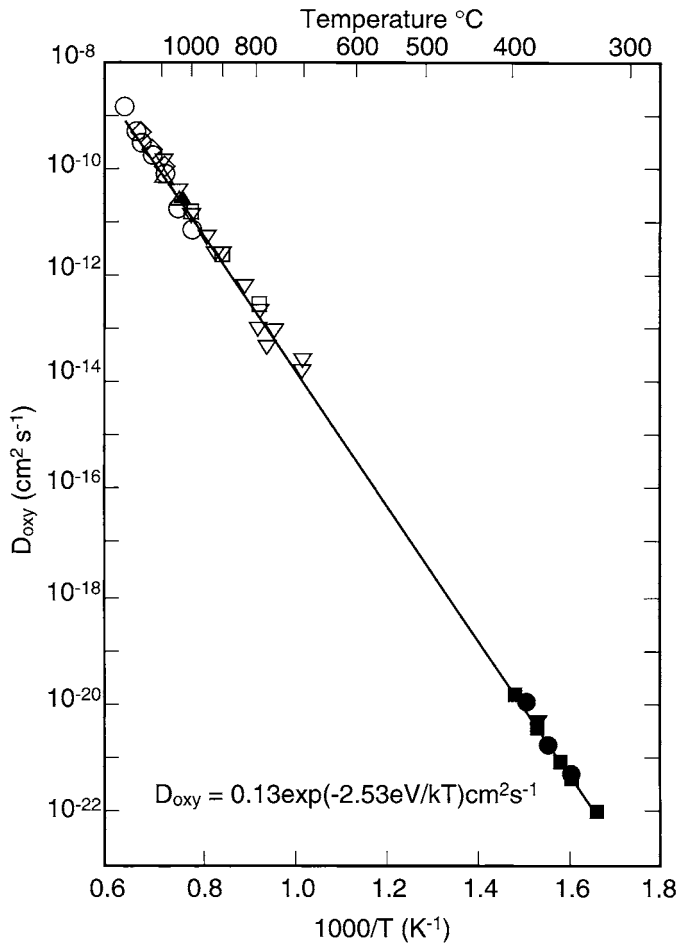

Figure 2. Measured values of 'normal' oxygen diffusion (D_{OXY}), together with a line fitted to the data by $D_{OXY} = 0.13\exp(-2.53\ \text{eV}/kT)\ \text{cm}^{-2}\ \text{s}^{-1}$. The data points for the high temperatures relate to measurements of SIMS profiles, except for the point (▲) that is obtained from internal friction measurements. The low temperature data refer to the relaxation of stress-induced dichroism (section 3.2). Further details are given in [13].

It is evident that the processes of diffusion and precipitation of O_i atoms in CZ Si are complex. It is more than 40 years since the publication of the first research papers on these topics and an enormous literature has now been built up while new papers continue to appear. The explanation for this pre-occupation relates primarily to the strong commercial interest associated with the increasing use of Si in the manufacture of integrated circuits that have ever decreasing feature sizes (currently $\sim$0.18 μm) and increasing complexity. There are also on-going intellectual challenges. The purpose of this review is to outline our current state of knowledge but also to indicate the areas where our understanding is still lacking.

The organization is as follows. We shall first discuss the lattice sites of oxygen atoms (section 2) and then show how measurements of single diffusion jumps established the concept of 'normal' oxygen diffusion over the wide temperature range 1325–330 °C (section 3). The results of long-range oxygen diffusion and the aggregation of these atoms at high, medium and low temperatures, that are more relevant to device applications, are outlined in sections 4–6.

We go on to show that at low temperatures diffusion of oxygen atoms can be enhanced by electron irradiation (the simultaneous introduction of vacancies and self-interstitials) or the introduction of hydrogen into samples: both H–O_i and H_2–O_i pair defects have been detected and characterized (section 7). Finally, TD(N) and STD(N) centres are discussed in section 8. Our conclusions are summarized in section 9.

2. The lattice sites of isolated oxygen atoms

Early infrared (IR) measurements of CZ Si made at room temperature revealed a broad absorption line at a wavelength λ close to 9 μm (1106 cm^{-1}) [24] with an absorption coefficient of $\alpha \sim 3\,cm^{-1}$ and a full-width at half-maximum $\Delta \sim 34\,cm^{-1}$ (see the profile on the right hand side of figure 3): this line is usually too small to be detected in FZ Si. At a sample temperature of 77 K, the line sharpens and shifts to 1136 cm^{-1}. In Si enriched with the ^{18}O isotope, added to the melt during crystal growth, a second line is observed at 1085 cm^{-1} [25]. The reduction of the vibrational frequency is expected since the frequency of a localized vibrational (LVM) mode of an impurity atom with a small mass is proportional to the inverse square root of the reduced mass (μ) of the oscillator. To a very close approximation, $1/\mu = [1/m_{imp} + 1/\chi M_{nn}]$ [26], where m_{imp} is the mass of the impurity (the O_i atom), M_{nn} is the mass of its nearest neighbours (Si atoms) and χ is a numerical factor (usually close to two) that depends on the geometry of the centre and the ratio of the local stretching and bending force constants [27]. A recent high resolution FTIR absorption spectrum [2] obtained at a temperature of 4.2 K from a sample containing enriched $^{17}O_i$ and $^{18}O_i$ is shown in figure 4: the natural abundances of the isotopes are $^{16}O_i$ (99.76%), $^{17}O_i$ (0.04%) and $^{18}O_i$ (0.2%). The line-widths are close to 1 cm^{-1}, and two relatively weak satellite features on the low energy side of each line, displaced by 1.9 and 3.8 cm^{-1} respectively, are due to the vibrations of oxygen atoms bonded to a naturally occurring ^{28}Si (92.3%) atom and a ^{29}Si (4.7% abundance) or ^{30}Si (3.0%) isotope, rather than to two ^{28}Si (92.3%) atoms [28, 29]. These observations lead to the unambiguous conclusion

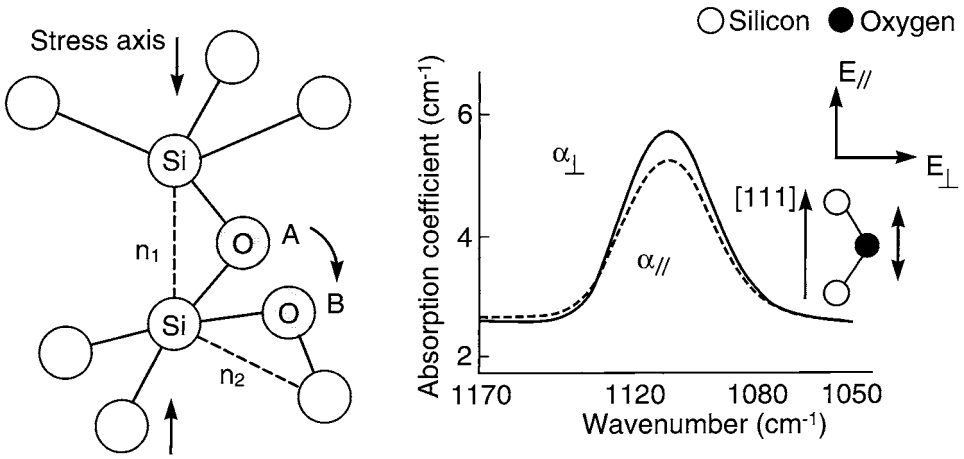

Figure 3. Diagram showing the effect of applying a static uni-axial stress to a CZ silicon sample along a [111] axis so that the concentration of O_i atoms n_1 decreases and the concentrations $n_2 = n_3 = n_4$ increase (left hand side). IR measurements of the broad 9 μm band at room temperature then show a smaller absorption coefficient with the E-vector of incident light polarized parallel to the [111] direction compared with the perpendicular polarization (right hand side). The difference is called the dichroism.

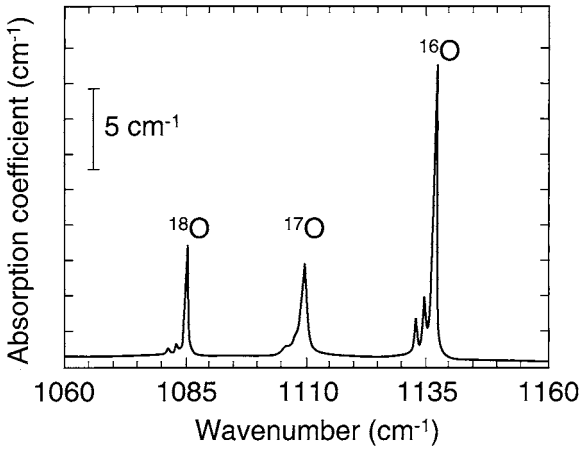

Figure 4. FTIR spectrum of a silicon sample (at 4.2 K) containing enhanced concentrations of $^{17}O_i$ and $^{18}O_i$, showing isotopic shifts of the associated LVMs to lower frequencies compared with that of $^{16}O_i$. The two weak satellites on the low energy side of each of the strong absorption lines are due to O_i atoms located between adjacent ^{29}Si–^{28}Si and ^{30}Si–^{28}Si isotopes, rather than a pair of ^{28}Si isotopes (see also figure 12). This is a modified diagram from [2].

that oxygen atoms occupy bond-centred interstitial sites in Si, as in silica (SiO_2). It is noted that the width (Δ) of the $^{17}O_i$ line (figure 4) is measurably greater than those of the lines due to the two other isotopes but there is currently no explanation.

Vibrating O_i atoms give rise to other IR absorption lines, some of which have been detected only recently by high resolution FTIR. The new observations have led to radical changes in the assignments of certain transitions, implying that the Si–O_i–Si structure is linear rather than bent as shown in (figure 1): the reader is referred to the literature for further details [30–32].

Considerable effort has been expended to establish measured calibration factors to convert values of the peak absorption coefficient α_{MAX} of the 9 μm band (300 K) to the concentration of isolated oxygen atoms [O_i] present in a sample: [O_i] is subsequently determined by a chemical or nuclear method. The calibrations have different labels according to their origin, e.g. ASTM (USA), New ASTM (USA), DIN (Germany) and important others from Japan: a comparison of some of these calibrations is given in [33]. In this article we shall use the calibration for which $[O_i] = 3.14\alpha_{MAX}$ cm^{-3} (Δ is assumed always to be 34 cm^{-1}) [34]. The loss of oxygen from solution resulting from the heat treatment of samples can therefore be quantified from the measured reduction in α_{MAX}, irrespective of the new locations of the atoms, provided the broad 9 μm IR band is not obscured by broader absorption from precipitated SiO_2. This problem can be overcome by making measurements at 4.2 K [2] when the 9 μm line becomes sharp (figure 4), whereas the absorption from silica precipitates remains broad [35]. Alternatively, absorption measurements can be made of an oxygen-induced mode at 19.5 μm (517 cm^{-1}) [36, 37] that is a resonance near the top of the phonon dispersion at 520 cm^{-1} of the perfect silicon lattice [38, 39]. Measurements can only be made on very thin samples if they are doped with either donors or acceptors at concentrations of $\lesssim 10^{17}$ cm^{-3}. More highly doped substrate material ($\sim 10^{19}$–10^{20} cm^{-3}) is opaque because of the resulting strong free-carrier electronic absorption.

3. Measurements relating to *single* oxygen diffusion jumps

Diffusion of O_i atoms occurs by atomic jumps from a bond-centred site to one of the six equivalent adjacent sites with a jump distance $d = (2)^{1/2}a_0/4 = 1.92$ Å (figure 1), where

$a_0 = 5.42$ Å is the lattice spacing of Si. D_{OXY} is equal to d^2/τ, where τ is the mean lifetime for a jump to occur. τ is given by $\tau_0 \exp(E_D/kT)$ at a temperature T, where E_D is the activation energy. Thus $D_{OXY} = D_0 \exp(-E_D/kT)$, with $D_0 = a_o^2/8\tau$. The lowest observed value of D_{OXY} at a given temperature is taken to define 'normal' diffusion.

Under equilibrium conditions, the bond-centred sites along the four ⟨111⟩ directions are equivalent in a strain-free crystal and the four populations n_1–n_4 of O_i atoms (figure 1) are equal. If the crystal is subjected to a uniaxial stress, these populations become unequal, provided the temperature is sufficiently high for diffusion jumps to occur. This is because some bonds are extended and others are shortened, making the energies of inserting an oxygen atom smaller and greater, respectively. The dynamics of the resulting concentration changes, their reversal resulting from a reversal of the stress, or their decay once the stress is removed have been analysed to obtain values of D_{OXY} at the microscopic level for heat treatments at both high and low temperatures. The measured time constants for these processes are given by $\tau^* = \tau/8$ and D_{OXY} is therefore equal to $a_o^2/64\tau^*$. Details relating to the numerical factor of 8 that takes account of the bond-centred geometry of the O_i site are given in [13].

3.1. High temperatures (1325 > T > 850 °C)

In the earliest work, acoustic waves with frequencies of 100 kHz or 300 kHz (angular frequencies, ω) were used to generate an oscillating stress in a heated block of Si [40, 41]. As the temperature was raised progressively, damping of the waves occurred with a broad superposed resonant peak at the temperature when $\omega\tau^* = 1$. The evaluation of τ^* and an analysis of the shape of the curve [42] provided sufficient information to determine values of

$$D_{OXY} = 0.21 \exp(-2.55 \text{ eV}/kT) \text{ cm}^2 \text{ s}^{-1}$$

that are essentially indistinguishable from the expression given in section 1. These measurements were also the first to validate proposals that O_i atoms occupy bond-centred sites with ⟨111⟩ axes.

The reader is referred to the original papers for details of the experimental procedures and their interpretation since these are outside the scope of the present article. We note only that the techniques are analogous to those used in the measurements of the diffusion coefficients of interstitial carbon or nitrogen impurities in body-centred α-Fe [14, 43].

3.2. Low temperatures (400 ⩾ T ⩾ 330 °C)

Measurements made in this low temperature range involve a different procedure that is very precise [44, 45]. If a sample is subjected to a *static* uniaxial stress of ∼100 MPa along a [111] direction for 15–30 min at 400 °C (left hand side of figure 3) and then cooled to room temperature with the stress still applied, n_1 is smaller than $n_2 = n_3 = n_4$ and this distribution is frozen in. The absorption coefficient, $\alpha_\parallel$, of polarized light with the E-vector parallel to the stress axis is then smaller than, $\alpha_\perp$, with the E-vector perpendicular to the [111] axis (the right hand side of figure 3). The normalized dichroism $3(\alpha_\perp - \alpha_\parallel)/(\alpha_\parallel + 2\alpha_\perp) \sim (\alpha_\perp - \alpha_\parallel)/\alpha_\perp$ decays exponentially with the measured time constant τ^* during a subsequent isothermal anneal. Measurements made on several samples at different temperatures lead directly to the values of D_{OXY} shown in figure 2. Other low index stress and viewing axes (⟨100⟩, ⟨110⟩ and ⟨111⟩) can be used as discussed in [45].

In summary, the available measurements [40–42, 45–47], leading to the values of D_{OXY} (figure 2), define a single mechanism for 'normal' diffusion of O_i atoms in Si over some 14 decades for the temperature range 350–1300 °C. It is unfortunate that there are no corresponding

data for the range, $400 \leqslant T \leqslant 850\,^{\circ}\mathrm{C}$, since less direct measurement techniques have indicated that enhanced diffusion may occur (section 5).

4. Oxygen diffusion and precipitation ($1400 \geqslant T \geqslant 700\,^{\circ}\mathrm{C}$)

4.1. Oxygen in- and out-diffused profiles

High temperature in-diffused $^{18}O_i$ [48, 49] and out-diffused $^{16}O_i$ [50, 51] distributions of oxygen in Si, measured by SIMS, have been satisfactorily fitted to error function profiles and the derived values of D_{OXY} are in excellent agreement with the results of the damping of acoustic waves at similar temperatures (section 3) (figure 2). The in-diffusion measurements also yield values of the oxygen *surface* concentration (c_s) that correspond to the oxygen solubilities measured by other methods (figure 5) [35, 52]. Other SIMS measurements have been reviewed in [12], [13] and [53]. There is evidence from IR measurements [54, 55] that grown-in carbon atoms complex with O_i atoms to form C(3) centres (C_i–O_i pairs) [56, 57] that act as nuclei for oxygen precipitation (section 4.2) so that diffusion profiles are modified. There is also evidence that the rate of oxygen diffusion at 750 °C is enhanced by a factor of ~10 in samples containing a high concentration of carbon. It was proposed that rapid correlated jumps of the two atoms occur [58], similar to those of the two interstitial oxygen atoms present as dimers (section 6).

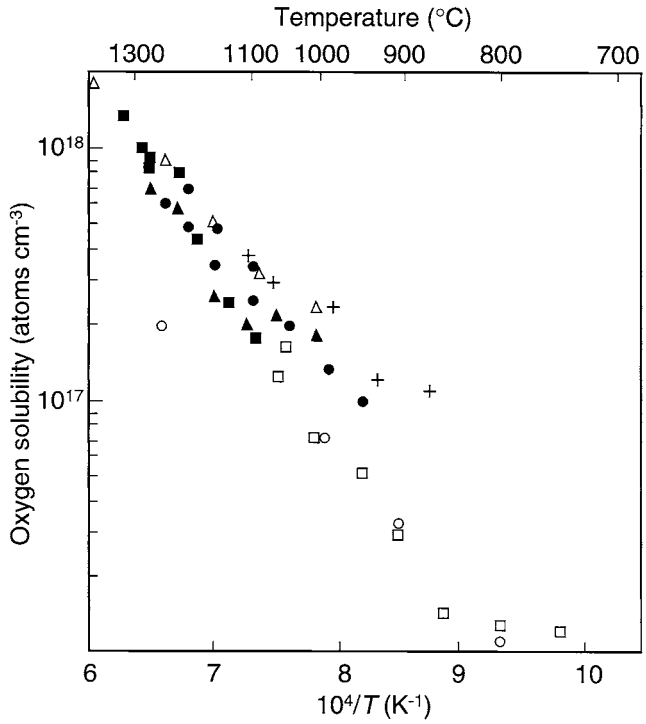

Figure 5. Collected data for the solubility of interstitial oxygen atoms in silicon at high temperatures, shown as an Arrhenius plot: details of the individual measurements are given in [35] and [52].

4.2. Oxygen precipitation

When CZ Si is annealed at temperatures, $T > 700\,^{\circ}$C, there is growth of small SiO_2 precipitates nucleated during a prior low temperature heat-treatment that may be the cooling period following crystal growth: alternatively, the nucleation may be due to grown-in carbon or other impurity atoms (section 1). The rate of growth of the SiO_2 precipitates can be quantified straightforwardly provided O_i diffusion is the limiting process [35, 59–62]. In the early stages, the number of O_i atoms per unit time that cross a spherical surface surrounding a diffusion sink with a capture radius r_c is given by $4\pi c_0 r_c D_{OXY}$, where c_0 is the grown-in oxygen concentration, $[O_i]_0$. If r_c is set equal to the radius r_p of a growing (approximately spherical) precipitate, we obtain $r_p^2 = (2c_0 D_{OXY}/c_p)t$, where $c_p = 4.6 \times 10^{22}$ cm^{-3} is the concentration of oxygen atoms in SiO_2. c_0 is initially significantly larger than the equilibrium solubility, c_s, but after a long anneal it decreases towards c_s and a sample temperature of 4.2 K must be used to obtain reliable IR measurements. The number density of precipitates $n(T)$ can be determined by counting etch pits produced by chemical etching and their size can be measured by transmission electron microscopy (TEM) or, non-destructively, by small angle neutron scattering (SANS) from bulk material [35]. The two methods give equivalent results [63], yielding values of D_{OXY} corresponding to 'normal' diffusion (sections 3 and 4.1). It is implied that long-range diffusion of O_i atoms controls the rate of growth of the precipitate particles for $T > 700\,^{\circ}$C, rather than the interface reaction involving the formation of I atoms required to accommodate the local increase in volume. This conclusion has been verified by measurements discussed in [64]. Diffusion and aggregation of the generated I atoms leads to the formation of stacking faults [14] but the local build-up of stress may also lead to the formation of small punched-out prismatic dislocation loops adjacent to the SiO_2 precipitates [65]. Both defects are essentially immobile and they act as sites for further precipitation of oxygen atoms.

As the anneal temperature is lowered, $n(T)$ *increases* due to the increasing oxygen supersaturation. For a sample with $[O_i] \sim 1.5 \times 10^{18}$ cm^{-3}, it has been shown that $n(T) \sim 6 \times 10^{-3} \exp(+3\text{ eV}/kT)$ cm^{-3} [13, 66]: somewhat lower temperature dependencies are found for samples with smaller grown-in oxygen concentrations. To achieve conservation of oxygen atoms, the 'radius', r_p, of the particles must be proportional to $n(T)^{-1/3}$ that has a temperature dependence given by $\exp(-1.0\text{ eV}/kT)$. It follows that an Arrhenius plot of the rate of loss of O_i atoms from solution with normal diffusion will have a gradient of only -0.5 eV, corresponding to that of the triple product $r_p n(T) D_{OXY} \propto n(T)^{2/3} D_{OXY}$.

The precipitation process is reversible so that there is partial dissolution of existing SiO_2 particles during a second anneal at a higher temperature. The new equilibrium concentration of dissolved O_i atoms can then be identified with the oxygen solubility at this temperature. Unfortunately, there are difficulties in comparing values reported by various investigators because of their use of (a) different sample temperatures to determine the strength of the 9 μm oxygen band and (b) different calibration factors to convert the absorption coefficients into oxygen concentrations [35]. The parameters used have varied by a factor of two or more throughout the period of studies and the particular value used was not always clearly stated. Nevertheless, these estimates of the solubilities (figure 5) are in general agreement with those measured at the surface by SIMS after in-diffusion of oxygen ($^{18}O_i$) [12]. This correlation implies that surface effects, such as the in-diffusion or out-diffusion of I atoms, vacancies or unknown impurity atoms are unimportant in relation to the oxygen solubilities at high temperatures. We note, however, that extended anneals lead to continued growth of the larger precipitate particles and a progressive loss of the smaller particles due to their dissolution [63]. This process, that is well known in metallurgy, minimizes the total interface energy of the system and is called Ostwald ripening.

It is important to recognize that nucleation sites identified with boron or carbon atoms cannot be removed during the early stage of the anneal in contrast to the dissolution of small SiO_2 particles. Since the grown-in substitutional impurity atoms have small covalent radii, the local strain is expected to be reduced by the capture of interstitial oxygen atoms.

The maximum rate of trapping of mobile Fe (or other impurity atoms) is $4\pi n(T) r_p D_{Fe}$, where D_{Fe} is the diffusion coefficient of Fe atoms. The sticking probability of the Fe atoms will depend on the particle size and the anneal temperature. Since small particles are not the most effective and large particles will have a low concentration, the size must be optimized at an intermediate value as discussed in [8].

5. Oxygen diffusion and precipitation ($650 \geqslant T \geqslant 430\,^{\circ}C$)

5.1. Diffused profiles: a fast diffusing species

The values of D_{OXY} at temperatures in this range were thought originally to be too small to allow out-diffusion of oxygen to be detected from SIMS profiles. To obtain reliable measurements, the depletion depth from the surface has to be in the range 5–10 μm. Nevertheless, reports of observed out-diffusion have been reviewed and confirmed in a recent extensive re-investigation [53] of samples annealed for different temperatures for times of up to 170 days. The measured profiles are strange because their depths ($\sim$5 μm) are essentially independent of the anneal temperature, and increasing the anneal time leads only to slightly larger reductions in the surface concentration. Consequently, if the profiles are fitted to an error function distribution, the derived diffusion coefficient, D_{EFF}, is essentially constant over this whole temperature range. It could therefore be implied that there is an 'enhancement' of D_{OXY} that increases progressively by a factor of up to $\sim 3 \times 10^5$ as the temperature is lowered from 650 °C to 450 °C (figure 6). Reductions in the concentrations of *isolated* O_i atoms in the bulk of the samples, determined by IR absorption measurements, were found to be correlated with the reductions in the surface oxygen concentrations (SIMS), even when O_i diffusion was enhanced by introducing hydrogen into samples in a pre-treatment (section 7.3). It was concluded that there is conversion of some O_i atoms to a fast diffusing species, O_{fds}, that can migrate over large distances as a stable entity before being trapped at the surface or in the bulk. The diffusion depth revealed by SIMS can then be associated with this distance. The formation of an O_{fds} has been proposed previously in relation to out-diffusion [67], in-diffusion [68], internal oxygen clustering [69] and the transformation of TD(1) to TD(2) [70]. The new results [53] provide no evidence for the dissociation of O_{fds} in the temperature range 450–500 °C, consistent with previous data for higher temperature anneals at up to 700 °C. Possible identities of the O_{fds} defect will be discussed in section 7.

5.2. I-atom aggregation during annealing

Anneals of CZ Si in this temperature range lead to the formation of 'ribbon-like defects' (RLDs) with a ⟨311⟩ axis that are revealed by direct TEM lattice images. The defects were initially attributed to coesite, a high pressure phase of silica [71], following analyses of optical diffraction patterns of the TEM images. Measurements of the number density of these defects, together with estimated numbers of oxygen atoms incorporated in individual particles, led to the conclusion that D_{OXY} would have had to be enhanced by a factor of $\sim 10^4$ at 485 °C [72]. Observation of TEM contrast does not, however, necessarily imply that the defect responsible incorporates oxygen atoms. By contrast, RLDs were not detected by SANS measurements, implying the absence of coherent n^0 scattering from the nuclei of clustered oxygen atoms

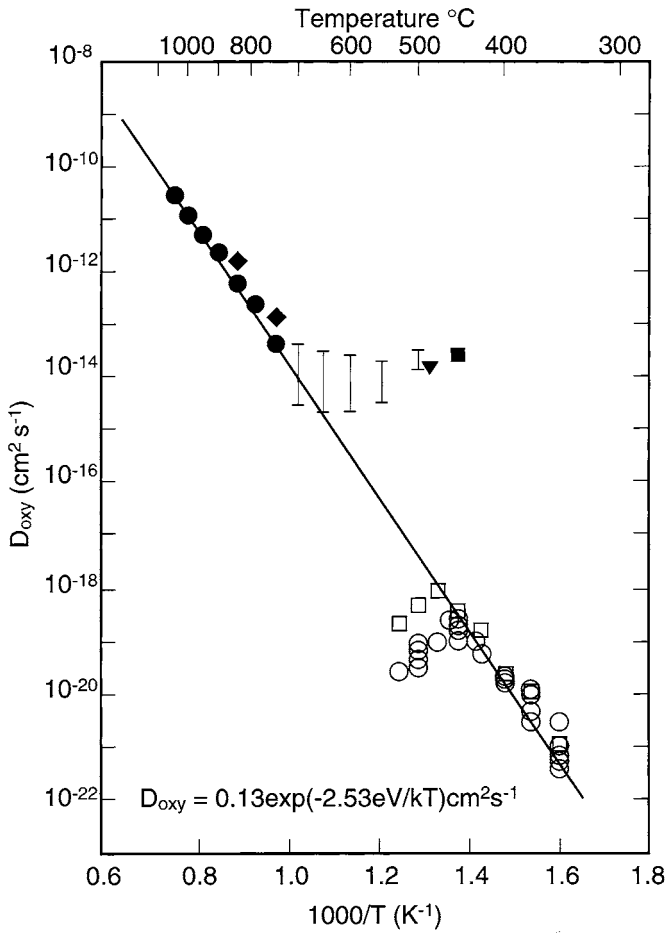

Figure 6. An Arrhenius plot of data for the diffusion coefficient of oxygen atoms in silicon deduced from in-diffusion, out-diffusion and precipitation measurements, indicating enhanced values of D_{OXY} in the temperature range 500–650 °C and reduced values just above 450 °C as discussed in the text: details of the individual measurements are given in [35] and [80].

[35]. The interpretation was therefore questioned and it was proposed instead that 'black dot contrast', that was also detected by TEM, should be identified with very small SiO_2 particles [52]. Later TEM studies, incorporating energy loss measurements, confirmed that RLDs contained only very small concentrations of oxygen (∼5%) and the RLDs were reassigned to hexagonal Si [73]. This interpretation has been further modified and it is now accepted that the defects are local regions of silicon that are re-bonded as a result of clustering of I atoms formed during the growth of the SiO_2 particles (section 1) [74, 75]. This explanation is consistent with the observation by TEM of very similar structures observed in FZ Si after high energy electron irradiation (∼2 MeV) that generates I atoms and vacancies. Thus, the growth of RLDs does not imply enhanced O_i diffusion but does imply generation, diffusion and aggregation of I atoms. Measurements in progress at the Institut Laue–Langevin (ILL) at Grenoble using SANS, that now have a much improved sensitivity [76], should yield further direct information about the rate of growth of very small oxide precipitates and demonstrate whether or not there is evidence for enhancements of D_{OXY}.

5.3. Kinetics of O_i *aggregation and solubility*

As the anneal temperature is lowered from ∼600 °C, the size of SiO_2 particles decreases and there are changes in the precipitation kinetics. The slope of an Arrhenius plot of $d[O_i]/dt$, initially −0.5 eV, decreases to zero (550 °C), then becomes *positive* before becoming zero again (470 °C) and finally becomes negative with a value of approximately −2 eV for all values of $T < 450$ °C [13, 66]. The measured gradients vary according to the grown-in oxygen concentration, $[O_i]_0$, indicating that these energies are *not* activation energies but averages for a range of cluster sizes. The changes in the slope have been attributed to the change from a macroscopic to a microscopic (atom by atom) precipitation process [52]. At the higher temperatures, the capture radius for diffusing O_i atoms is identified with the large increasing radius of the precipitate particles, whereas at lower temperatures the particle radius becomes comparable with, and then smaller than, the capture radius. Calculations made with the assumptions of a constant capture radius of $r_c \sim 5$ Å, together with 'normal' O_i diffusion imply that the average number of O_i atoms incorporated per precipitate particle ranges from 100 to 20 for anneals in the temperature ranging from 600 to 500 °C [52].

As the anneal temperature is lowered to 700 °C, the 'derived' oxygen solubility decreases and then passes through a broad minimum with a value of $\sim 10^{16}$ cm^{-3} (see figure 5) but then increases to $\sim 2 \times 10^{17}$ cm^{-3} at 500 °C. It was inferred originally that this behaviour resulted from the large increase of the interfacial energy as the precipitates became ever smaller [13]: a later alternative proposal is that ejection of I atoms from small precipitates is inhibited, leading to a high supersaturation of O_i atoms due to the build-up of strain [77]. Although both processes may occur, there is spectroscopic evidence from high resolution photo-luminescence (PL) measurements for I atom generation at somewhat lower temperatures [78], since interstitial carbon atoms are produced.

As a final comment, a single maximum oxygen nucleation rate with decreasing temperature is expected on the basis of classical nucleation theory but two maxima are observed at $T \sim 750$ and 500 °C, respectively [79]. This behaviour is currently unexplained but may also relate to a change from macroscopic to microscopic kinetics as the temperature is lowered.

6. Oxygen aggregation and thermal donor formation ($T \leqslant 500$ °C)

The first stage of oxygen aggregation is the formation of O_2 dimers in material that contains essentially only isolated O_i atoms. The rate of loss of O_i atoms from solution would then be given by $d[O_i]_t/dt = -8\pi r_c D_{OXY}[O_i]^2$: the numerical factor of 8, rather than the usual value of 4, is required since both oxygen atoms diffuse [80]. Integration of this equation leads to the relation $(1/[O_i]_t) = (1/[O_i]_0) + 8\pi r_c D_{OXY} t$, where $[O_i]_0$ and $[O_i]_t$ are the concentrations of dissolved oxygen atoms at the start of the anneal and after time t, respectively. Any O_i atom can be trapped by any other O_i atom (10^{18} cm^{-3}) but the loss of O_i atoms due to trapping by carbon or other impurity atoms (contamination) at concentrations of $\sim 10^{16}$ cm^{-3} is negligible. Since $[O_i]$ can be measured by IR absorption after successive periods of annealing, it is possible to determine values of D_{OXY} for temperatures as low as 350 °C, again assuming that $r_c = 5$ Å (figure 6). Derived values of D_{OXY} are independent of the initial value of $[O_i]_0$ for anneals at 350, 375 and 400 °C but they are greater by a factor of three to four than the values determined from the relaxation of stress-induced dichroism [80].

The kinetic equation used above takes no account of dimer dissociation or of the formation of larger oxygen clusters. The dissociation rate of dimers is expected to increase as the anneal temperature increases so that measured values of $[O_i]_t$ after the anneal are expected to be greater than those calculated, especially for samples with a low value of $[O_i]_0$. This behaviour

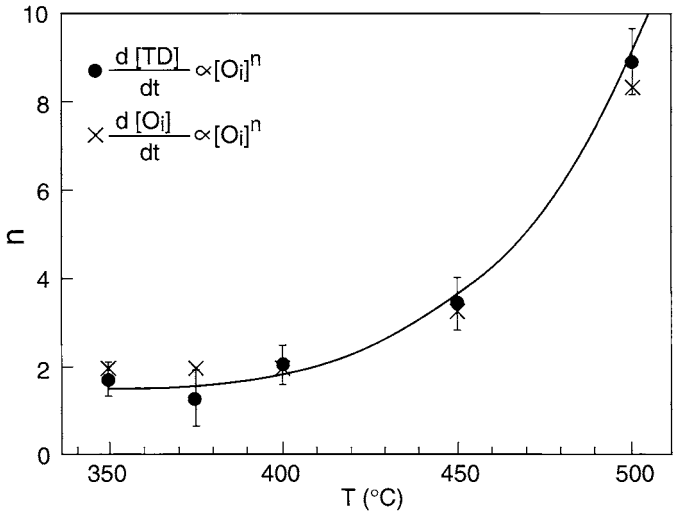

Figure 7. The power dependency n of the initial rates of thermal donor formation (●) and loss of O_i atoms from solution (×) in CZ Si as functions of the anneal temperature [80]. The value of $n = 4$ (only appropriate for 450 °C) was, until recently, assumed to be the same for all temperatures, implying that the aggregation of four O_i atoms led to the formation of a thermal donor. It is now clear that O_2 dimers constitute the first essential step and that the increasing values of n, as the temperature is increased, are related to dissociation of small oxygen clusters.

is apparent for anneals at 450 °C and, more particularly, at 500 °C where the derived values of D_{OXY} are all much too small (figure 6) [80]. These effects are revealed by assuming that the initial values of $d[O_i]/dt$ are proportional to $[O_i]^n$. A plot of n versus T (°C) shows that n increases from 2 ($T = 400$ °C) to ∼10 ($T = 500$ °C) (figure 7). These results are mirrored by the rates of formation of thermal donor centres TD(N) (section 8) that have been attributed to small oxygen clusters aligned along ⟨110⟩ axes and are thought to incorporate one extra oxygen atom as the index N increases to $(N + 1)$ [21, 22]. Early work [24], relating to anneals carried out at 450 °C, led to the proposal that all TD(N) centres incorporate *four* oxygen atoms since their rate of formation was proportional to $[O_i]^4$. This dependency is in agreement with the more recent analysis but only for this one temperature. A dependency of $[O_i]^2$ at lower temperatures, however, indicates that dimer formation must be the rate limiting step.

The evolution of the concentrations of larger oxygen clusters, with three, four, five etc atoms, as a function of anneal time can be simulated from a numerical integration of coupled differential equations [81], rather than the single equation discussed above for dimers. With the assumption that only single oxygen atoms are mobile and that there is no dissociation of clusters, the concentrations $[O_2]$, $[O_3]$ and $[O_4]$ etc decrease sequentially by factors close to ten for every additional oxygen atom added to a cluster during simulated anneals at 450 °C for times of up to ∼100–200 h (figure 8). This prediction is inconsistent with the much smaller relative concentrations (figure 9) observed of TD(N) centres with adjacent values of N [21, 22]. In addition, many workers had proposed that there is a large enhancement of D_{OXY} by factors ranging up to $\sim 10^4$ [24, 69]. Such an increase would, however, lead to an impasse since there would be a huge discrepancy with measurements of the rate of O_i loss from solution. This was not recognized in the early work as these measurements were not made.

We next consider the thermal stability and diffusion of O_2 dimers, that are thought to diffuse more rapidly than O_i atoms by a factor of up to 10^7 [82, 83]. If the time constant for

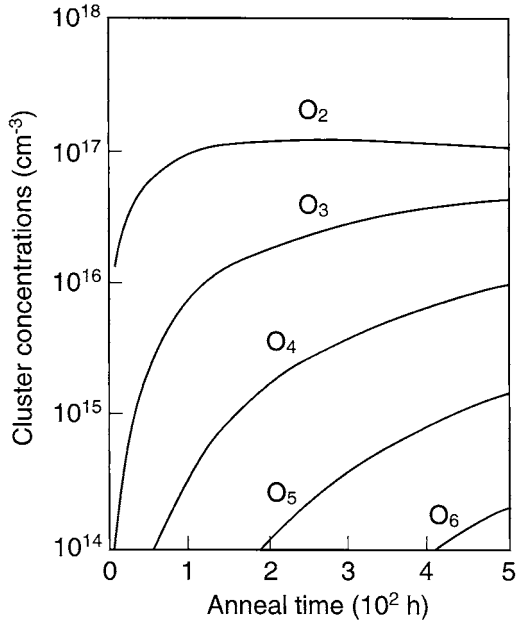

Figure 8. The serial growth of oxygen clusters O_2, O_3, O_4 etc as a function of annealing time for a simulated anneal at 450 °C with the normal value of D_{OXY}, assuming O_2 dimers are immobile and that there is no dissociation of the clusters [81].

dissociation is greater than the time for a diffusing dimer to be trapped by an isolated O_i atom, a trimer will be formed. The concentration of trimers then corresponds closely to the original rate of formation of dimers but dissociation of O_3 centres to reform an O_i atom and a dimer (over a longer period of time) would also allow the relatively rapid formation of O_4 and O_5 defects. The dissociation of these larger clusters, again with the release of dimers, would allow even larger clusters to be formed but without the further loss of isolated O_i atoms [80, 84]. Such processes have been shown to overcome the previous impasse of connecting the growth of TD(N) centres (with high values of N) to the formation of oxygen clusters with increasingly large sizes: further discussion of TD(N) centres is given in section 8.

There is convincing evidence for the formation of dimers with a binding energy ∼0.3 eV and concentrations of up to $\sim 10^{14}$ cm^{-3} derived from recent IR LVM measurements made on samples containing various relative concentrations of ^{16}O and ^{18}O that were analysed by density functional calculations [85–88]. The two atoms occupy second neighbour bond-centred sites and there is no evidence for the ejection of an I atom: other theoretical analyses have also implied that rapid diffusion occurs [89–92]. Rapid diffusion of dimers does not, however, explain all the observations. For example, the slope of an Arrhenius plot for the evolution of the TD(N) centres is close to 1.8–2.0 eV (see the lower temperature points in figure 6) [93] that does not correspond to the activation energy for normal oxygen diffusion (2.5 eV) that should be the rate limiting process. A suggestion that trimers and larger oxygen clusters are also mobile appears to assist the overall interpretation [85] although there is no direct evidence for the migration of large complexes. Nevertheless, TD(N) defects have been shown to re-orient (rotate) due to the application of a uniaxial stress [94, 95] and so the possibility of diffusion of 'oxygen clusters' cannot be ruled out. The re-orientation kinetics are not exponential but the characteristic energy is close to 2.7 eV [95], similar to that of 2.5 eV for normal O_i diffusion.

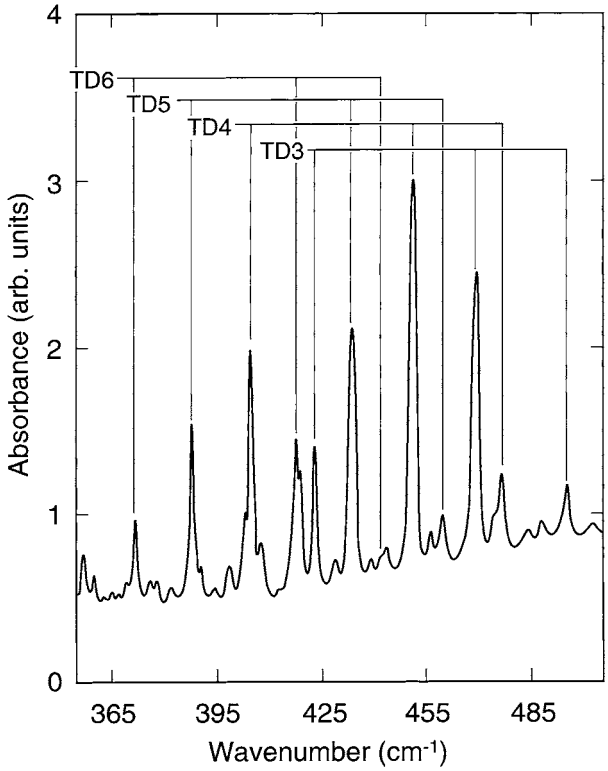

Figure 9. Electronic transitions of the sequence of TD(N) centres formed during an anneal at 470 °C, showing the progressive reductions in their ionization energies, E_i. It is also demonstrated that the donors have comparable concentrations as N is increased to (N + 1), (N + 2), etc.

A somewhat higher energy for the reorientation is not surprising since there must be local dissociation of O_i atoms from the aggregate to allow diffusion jumps to occur.

7. Mechanisms of enhanced oxygen diffusion

Enhanced O_i diffusion has been attributed to transient pairing of O_i atoms with diffusing vacancies, self-interstitials or a second impurity atom that reduces the height of the barrier for O_i diffusion jumps. *Ab initio* calculations are helpful in assessing possible mechanisms but experiments are needed to identify unambiguously the paired species. A discussion has already been presented in section 6 relating to the formation and diffusion of the O_2 dimer, and possible interactions of O_i atoms with interstitial carbon atoms were included in the discussion given in section 4.1. Proposed interactions involving oxygen–vacancy (V–O) pairs, I–O pairs, metal–oxygen pairs or hydrogen–oxygen pairs are now examined.

7.1. 2 MeV electron irradiation producing V–O_i and I–O_i centres

High energy electron irradiation of Si generates interstitial atoms and vacancies. The vacancies are mobile and are trapped by O_i atoms to form V–O_i pairs (A centres) that are stable up to $T \sim$ 250–300 °C. These defects are well characterized by both EPR [96] and IR [97] measurements that reveal an LVM at 835 cm^{-1} for the neutral defect. The resulting

'substitutional' oxygen atom is displaced along a ⟨100⟩ direction and is bonded to two nearest neighbours: the other two Si neighbours interact with each other by a weak anti-bonding orbital, leading to a defect with C_{2v} symmetry. Negatively charged centres have the same symmetry but the LVM shifts to 884 cm^{-1} [98]. These two LVMs have the same IR calibration factor as that for isolated O_i atoms, allowing the A-centre concentrations to be determined [98, 99].

Information about I–O_i pairs has been obtained from IR measurements [13, 100] (LVMs at 956 and 935 cm^{-1}), EPR [101] and theory [102]: these defects dissociate at $T \sim 50\,^{\circ}C$ and measurements indicate that they also have the same IR calibration factor as isolated O_i atoms [13, 103].

The effect of electron irradiation on samples containing O_i atoms aligned by the prior application of a uniaxial stress is easily understood. Once the vacancy has been captured, all knowledge of the O_i alignment axis is lost since re-orientation of A centres occurs at room temperature [96, 97]. The subsequent capture of an I atom, that is predicted from modelling of the damage process [104], allows the O_i atom to be located in any of the four bond-centred sites [105] (figure 1). The overall process therefore leads to a loss of dichroism (section 3.2) with a 75% probability. The involvement of the vacancy is confirmed experimentally since the rate of loss of the dichroism is reduced by a factor of ∼6 in irradiated Si containing neutral substitutional tin impurities (10^{19} cm^{-3}) [106] that are efficient traps for vacancies at temperatures of up to $T \sim 150\,^{\circ}C$ [107, 108]. The rate of loss of dichroism increases super-linearly during irradiation of samples at $T > 300\,^{\circ}C$ [109]. It could be inferred that there are transient interactions (collisions) between O_i atoms and mobile vacancies or I atoms since A centres are not stable in this temperature range.

Isothermal annealing of irradiated silicon leads to an initial increase in the concentration of isolated O_i atoms [13, 110, 111] that can be simply explained if A centres capture diffusing I atoms released from small clusters of these defects generated during the irradiation (precursors to RLDs: section 5.2): we designate this as process 1. In a second stage of the anneal, the concentration $[O_i]$ neither decreases nor increases. In this stage there is, however, the formation of a new centre that gives rise to an IR line at 889 cm^{-1} (77 K). The line has been attributed to a V–O_2 defect that is formed by the diffusion and the subsequent capture of an A centre by an isolated O_i atom that would lead to a decrease in $[O_i]$ (process 2). If processes 1 and 2 both occurred in the second stage of the anneal, there could fortuitously be an explanation of the constant value of $[O_i]$. Nevertheless, an Arrhenius plot of the rate of loss of A centres during this latter process, using all the available data [110–112], leads to $1/\tau = (1/\tau_0)\exp(-2\ \mathrm{eV}/kT)$, with a value of $1/\tau_0$ in the range 10^{13}–10^{14} Hz (figure 10). This appears to imply that *single* atomic jumps occur, leading to a local rearrangement of these defects. Thus a clarification of the process of A centre annealing is still awaited.

In summary, it is possible to envisage transient interactions between O_i atoms and I atoms, as discussed in a previous theoretical paper [102], or between vacancies and O_i atoms that lead to enhanced O_i diffusion, but definitive experimental evidence in support of these proposals has not been obtained.

7.2. O_i–metal-atom pairs

Copper [113] and iron [7] interstitial impurities diffuse in Si, even at room temperature, and are easily introduced inadvertently during processing at elevated temperatures. It was proposed that collisions with O_i atoms led to enhanced oxygen diffusion, detected by the relaxation of stress-induced dichroism [114, 115]. The interpretation of the measurements was later found to be ambiguous since the samples were heated in quartz capsules together with the metal in

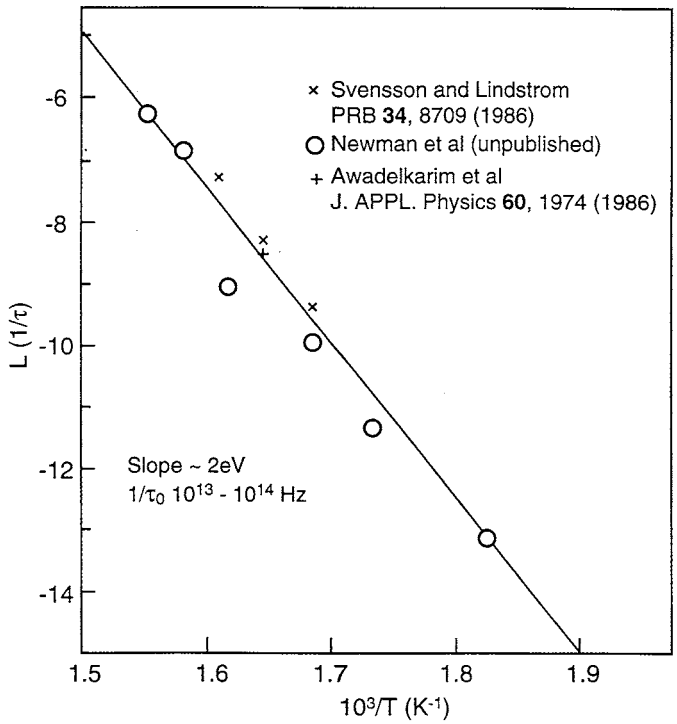

Figure 10. An Arrhenius plot of the rate of loss of V–O_i defects (A centres) as a function of the anneal temperature for CZ Si samples given a prior electron irradiation at room temperature. The time constant implies that only localized diffusion jumps occur [110]. A definitive explanation of the loss of A centres is still awaited.

the form of a hydrated salt. At that time, it was not recognized that the presence of hydrogen leads to enhancements, as discussed in the following section. It is important to note, however, that transition metals can catalyse the dissociation of H_2 molecules, as demonstrated for these impurities in germanium [116]. The increase in the concentration of atomic hydrogen would then be expected to increase the rate of O_i diffusion. Currently, it is therefore unknown whether or not direct metal–O_i interactions lead to enhanced O_i diffusion.

7.3. O_i–hydrogen-atom pairs

In 1957 it was reported that the rate of TD(N) formation in CZ Si grown in an atmosphere of hydrogen was ten times greater during a subsequent heat treatment at 450 °C than the rate in similar Si grown in the same equipment but in a helium atmosphere [117]. The implication that this was due to enhanced oxygen diffusion was not recognized and the work was ignored until relatively recently. In 1983, measurements of the relaxation of stress-induced dichroism of the 9 μm O_i band were made for Si that had been pre-heated in the growth chamber in a mixture of H_2 and Ar gases at 900 °C for 2 h. It was demonstrated unambiguously that D_{OXY} was enhanced for the range $250 \geqslant T \geqslant 350$ °C and the activation energy was reduced to ~2 eV [118] but there was still no explanation. It was only after another five years that it was demonstrated that the diffusion of hydrogen into Si was responsible for enhancing the rates of TD(N) formation [119] and the loss of dichroism of the 9 μm O_i band (figure 11) [120].

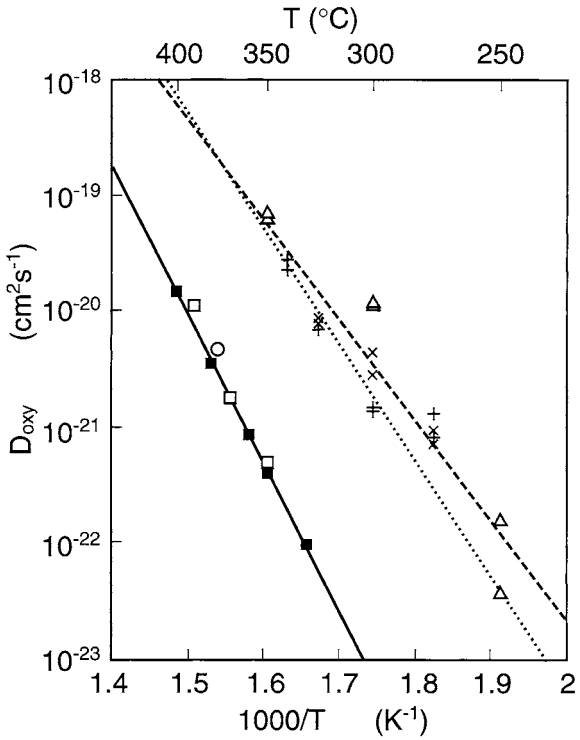

Figure 11. Arrhenius plot showing an activation energy of between 1.7 eV (dashed line) and 2.0 eV (dotted line) for O_i diffusion that is enhanced by the presence of hydrogen in the samples. The hydrogen was introduced by in-diffusion from H_2 gas during anneals at various temperatures in the range 800–1300 °C. The data for normal oxygen diffusion (solid line), shown for comparison, have an activation energy of 2.5 eV [80].

Hydrogen (or deuterium) may be introduced into samples by exposing them to a radio-frequency plasma (13.56 MHz, 1 bar, 40 W) while they are heated to a temperature in the range 150–500 °C [119, 120]: alternatively, samples may be heated to $600 \geqslant T \geqslant 1300$ °C in H_2, D_2 or a mixture of the gases [13]. Other procedures such as exposure of samples to HF acid or boiling water also introduces hydrogen into the surface region but they will not be discussed here. Recent measurements of the hydrogen (and deuterium) solubility, as functions of the temperature [121] and the pressure [122] of the gas (for the high temperature process) reproduce data derived by a different procedure in very early work [123]. The pressure dependence varies closely as $p^{1/2}$, implying that most of the hydrogen is introduced into the Si as atoms at high temperatures, so that the external gas molecules must dissociate at some stage. The temperature dependence of the total dissolved hydrogen is given by $[\mathrm{H}] = 9.1 \times 10^{21} \exp(-1.8\ \mathrm{eV}/kT)\ \mathrm{cm}^{-3}$, yielding concentrations of $\sim 10^{16}$ and $10^{14}\ \mathrm{cm}^{-3}$ at 1200 and 900 °C, respectively.

Subsequent examination of samples shows that a large fraction of the hydrogen is present as molecules that must form by diffusion and pairing of H atoms as the Si cools to room temperature. Some of the molecules form pairs with oxygen atoms, (H_2–O_i) [124], that dissociate on heating to $T > 40$ °C with the regeneration of O_i atoms and isolated H_2 molecules that have access to all the interstitial lattice sites [125]. These impurity defects are detected by IR absorption measurements and identified by replacing hydrogen by deuterium or mixtures of

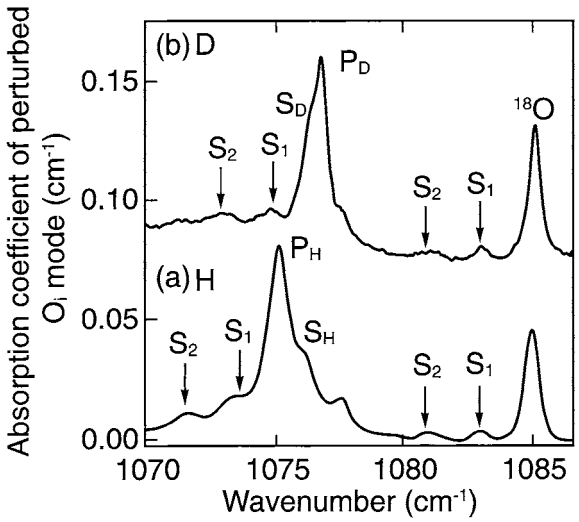

Figure 12. IR absorption spectra showing satellite lines S_1 and S_2 of isolated $^{18}O_i$ atoms, due to the formation of bonds to ^{29}Si and ^{30}Si, respectively: see also figure 4. The vibrational modes of $^{16}O_i$, complexed with (a) a hydrogen molecule (labelled P_H) and (b) a deuterium molecule (labelled P_D) also show these satellites demonstrating that the oxygen atom occupies a perturbed bond-centred site. The hydrogen molecules are formed during cooling of the silicon after the introduction of H or D atoms at 1300 °C from H_2 and D_2 gases [124]. The shift of the LVM to *higher* frequencies when H_2 is replaced by D_2 is unexpected since heavier atoms usually have lower vibrational frequencies: the reversal may be due to a level crossing process.

the two gases, that lead to shifts of the LVM frequencies (figure 12) [122, 124]. A discussion of the IR spectra and dipole moments (effective charge of $\sim 0.1\ e$) of the H_2 molecules, that have been attributed to interactions with the neighbouring Si atoms, is given in [124] and [126].

Isolated H_2 (D_2) molecules have also been observed by Raman scattering measurements following exposure of heated samples to a plasma [127, 128]. The location of these molecules in the crystal depends on the details of the procedure: there is now a consensus that the first H_2 centres reported [127] are located in small voids in the crystal but those reported in [128] are in interstitial lattice sites, as deduced from IR measurements.

The temperature at which the H_2 molecules dissociate is not known and so the concentration of hydrogen *atoms* at a given temperature is also unknown. This is important since the process of enhanced oxygen diffusion has been identified with interactions between O_i and hydrogen *atoms* [129–132]. This interpretation is supported by the detection of two types of H(D)–O_i pair by IR absorption following an anneal after *implantation* of H atoms into Si at 20 K: the centres dissociate at ∼200 K [133]. There is however a problem of reconciling this mechanism with the observations of enhanced O_i diffusion at 225 °C [124] since extrapolation of the hydrogen solubility relationship leads to only a negligible value of [H] $\sim 10^4$ cm^{-3}, whereas H_2 molecules may be present at concentrations of $\sim 5 \times 10^{15}$ cm^{-3}.

In this discussion it has been implied that D_{OXY} is enhanced only at temperatures up to about 500 °C following the prior diffusion of hydrogen into Si from H_2 (or D_2) gas at a high temperature. It has been inferred that there is in-diffusion of H atoms so that the barrier relating to the dissociation energy of the molecule (4.52 eV in free space and 3.9 eV in silicon [134]) must be overcome. It appears that this barrier limits the concentration of incorporated hydrogen to $\sim 10^{16}$ cm^{-3} at 1250 °C, since considerably higher concentrations

are easily introduced from a plasma of atomic hydrogen [127, 128]. Supporting evidence is provided by measured enhancements of D_{OXY} by a factor of 10^2 with increased hydrogen concentrations of up to 10^{19} cm^{-3} in the surface region of samples exposed to hydrogen gas at 1200 °C while they were subjected to 5 s pulses from a halogen lamp that emits UV radiation with an energy of up to ∼4 eV [135]. The limited depth of the enhancement was attributed to the penetration depth of the UV radiation. There is a need to repeat this work as rapid transient annealing is a standard procedure in device fabrication.

There is indirect evidence, from measurements of defect complexes by deep level transient spectroscopy (DLTS) [136] and the detection of electronic transitions from STDH(N) shallow thermal donors (section 8) [137], that small concentrations of hydrogen are often present in as-grown silicon. The hydrogen may be derived from water and/or organic materials present in ambient gases in the growth chamber or from polishing fluids.

8. Structures of double thermal donors TD(N) and shallow thermal donors STD(N)

Heat treatment of CZ Si in the range 350–500 °C, during cooling in the crystal grower or during a subsequent anneal, leads to the formation of two distinct types of donor, labelled TD(N) and STD(N) respectively, that are detected by IR absorption and EPR measurements. The two defects are related to each other and they have been attributed to the growth of small oxygen aggregates (section 6). We first discuss TD(N) centres, that comprise a family of more than 16 He-like double donors, and then show that there are at least three distinct families of STD(N) single donors.

8.1. TD(N) centres

TD(N) centres give rise to a series of sharp electronic IR absorption lines from their ground state (1s) to excited states ($2p_0$, $2p_\pm$, $3p_0$, $3p_\pm$ etc) that occur in the spectral regions 350–533 cm^{-1} (figure 9) and 580–1170 cm^{-1} from TD$(N)^0$ and TD$(N)^+$, respectively [21, 22]. As the anneal progresses, the family of donors evolves as the number of incorporated oxygen atoms per donor increases (increasing N). The ionization energies, $E_i(N)$ decrease, leading to shifts of the IR transitions to lower frequencies in the specified ranges. TD$(N)^+$ defects also give rise to an EPR spectrum labelled NL8 that is observed in samples partially compensated with grown-in boron, aluminium, gallium or indium acceptors: there is an unambiguous correlation with the IR data, deduced from studies of the stress alignment of the defects [138]. The g-tensor, derived from early EPR measurements made at X- or K-band frequencies, showed continuous changes of the g-values with increasing anneal time due to overlapping spectra from donors with decreasing localization [139]. Recent EPR measurements made at a microwave frequency of 140 MHz have now resolved the spectra of the individual centres and it has been shown that the symmetry of successive donors (an increase of N to $N + 1$) alternates from C_{2v} (orthorhombic) to C_s (monoclinic-1) [140, 141]. Electron nuclear double resonance (ENDOR) measurements confirm the incorporation of oxygen in TD(N) defects in samples containing enriched ^{17}O (nuclear spin $I = 5/2$) and naturally occurring ^{29}Si atoms ($I = \frac{1}{2}$) are also detected [142, 143]. There is no corresponding microscopic evidence from ENDOR for the incorporation of any other impurity, including (^{13}C, $I = \frac{1}{2}$), (^{14}N, $I = 1$), (^{10}B, $I = 3$), (^{11}B, $I = \frac{3}{2}$) and (^{27}Al, $I = \frac{5}{2}$).

The observations appear to be consistent with a model of TD(N) centres that have a central core structure consisting of two O_i atoms and a central I atom located in a row of O_i atoms aligned along a ⟨110⟩ direction (figure 13) [102]. If there are an equal number of oxygen atoms on each side of the core, the symmetry is C_{2v} but the addition of one extra oxygen

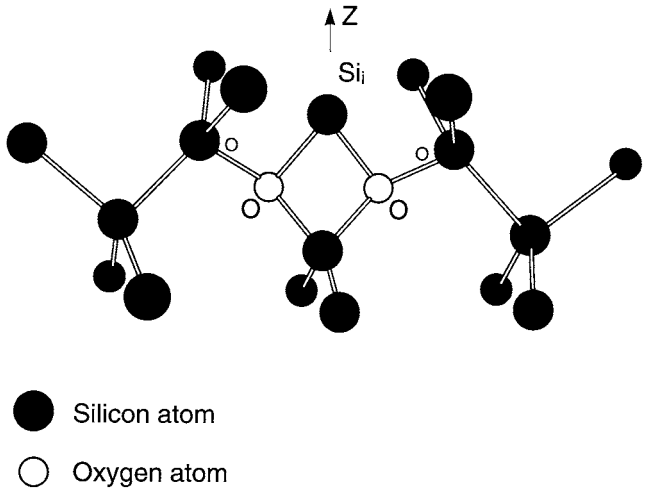

Figure 13. Proposed structure of the I–O_2 complex for the core of TD(N) centres, with unperturbed lattice positions marked by small open circles. In addition to the electrons present in bonds and lone pair orbitals, two electrons are delocalized so that the complex is a double donor [102].

atom at either end of the chain will lower the symmetry to C_s. It follows that the central I atom must make single diffusion jumps between adjacent oxygen atoms as N increases to $(N+1)$ and then $(N+2)$. The alternative possibility of adding O_i atoms alternately to the two ends of the chain seems improbable. Another possibility is that there is sequential addition of oxygen dimers, rather than O_i atoms, that would lead to the same changes of the symmetry. Irrespective of these details, the new magnetic resonance measurements explain the staircase structure revealed in a plot of measured values of E_i versus N (figure 14).

There is, in general, a consensus for the proposal of a row of O_i atoms in TD(N) centres but the structure of the core is still a matter for debate. For example, a recent first principles calculation has implied that neither vacancies nor self-interstitials *can be* present [144]. On the other hand, the proposal that an I atom is present in the core requires a demonstration that I atoms are generated during the period of growth of the donors. This process would relate to previous proposals [145, 146] that rapidly diffusing I atoms are generated by oxygen aggregation but it is not implied that all these aggregates are necessarily TD(N) centres or precursors to these centres. It is therefore important to seek experimental evidence for the formation of I atoms during low temperature anneals.

It is well known that I atoms are trapped by grown-in substitutional carbon atoms ([C_s] up to $\sim 10^{18}$ cm^{-3}), leading to their ejection into interstitial sites [C_i] [147]. The resulting loss of self-interstitials would then explain the observed reduced rate of TD(N) formation in highly carbon doped Si. The formation of di-carbon–oxygen–hydrogen defects (T centres), detected in hydrogenated Si by high resolution PL measurements provides direct evidence for the generation of interstitial carbon atoms [148, 149], adding weight to the detection of P centres with an O_2C_i structure, as discussed above [78]. A major shortcoming of PL measurements is that the strength of the emission cannot, in general, be converted into a defect concentration because of parallel recombination paths for the photo-excited holes and electrons.

Much earlier, however, EPR [150] measurements had shown that B, Al and Ga acceptors exchange sites with I atoms, introduced by 2 MeV electron irradiation (very recent theoretical work implies that boron atoms may not exchange sites with I atoms but that fast diffusing

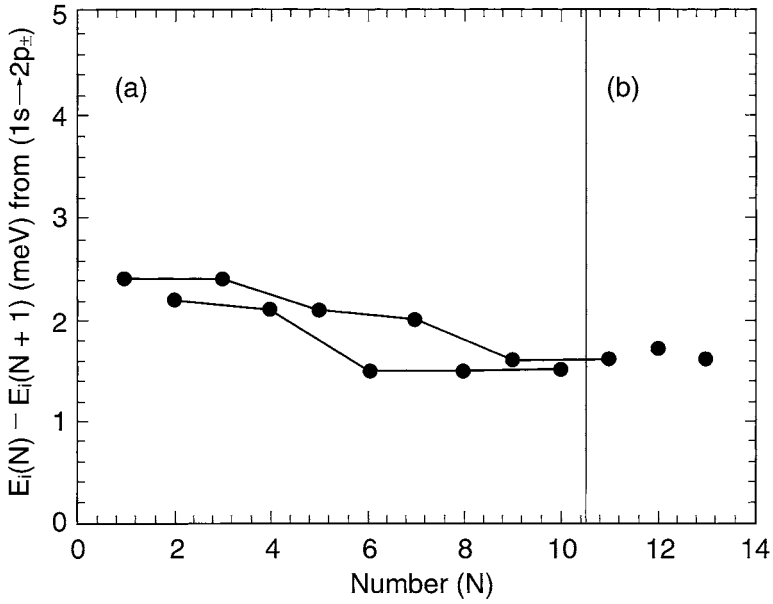

Figure 14. Diagram showing the differences of the ionization energies E_i of successive TD(N) centres, determined from the frequencies of the IR (1s $\rightarrow$ 2p$_\pm$) electronic transitions given in [21] and [22]. The resulting staircase structures, as N is increased to $N + 1$, etc imply alternating symmetries of adjacent centres, demonstrated directly by recent high resolution EPR measurements [140, 141].

close pairs form [151, 152] although that does not affect the discussion here). There are no reports for a similar exchange of sites for In acceptors but this is not expected because of their large covalent radius. Low temperature (77 K) IR LVM measurements also reveal the exchange of sites of boron atoms in irradiated Si [153] with the formation of lines from ^{11}Bi (730 cm^{-1}) and ^{10}Bi (757 cm^{-1}) and the subsequent generation of B–B pairs (believed to have C_{3v} symmetry) and larger B-interstitial clusters, as the anneal temperature is raised to 250 K and 300 K, respectively: the larger clusters dissociate only at $T > 300$–$400\,^\circ$C [154]. Measurements of the IR vibrational and electronic absorption lines from substitutional boron (both of which have measured IR calibrations), together with resistivity measurements, were then made on CZ Si ([B] $= 7 \times 10^{16}$ cm^{-3}) following anneals at 450 °C [155]. Derived values of [N_A] (LVMs) and [N_A–N_D] (electronic transitions) showed that there was a loss of boron from substitutional sites throughout the whole period of the anneal up to 2700 h (see also [156]) when the resistivity had increased from 0.28 Ω cm = 4.0 Ω cm (p type). It was deduced that the rate of TD(N) formation was similar to that for undoped Si but there was no evidence for the incorporation of boron in TD(N) centres. It was inferred that there was clustering of diffusing interstitial boron atoms: for every substitutional boron atom that was lost, there was a measured loss of ∼15 O$_i$ atoms. The ratio Δ[B]/Δ[O$_i$] is similar to that for Δ[C]/Δ[O$_i$] in samples with a carbon concentration of $\sim 10^{17}$ cm^{-3}. The important result is that these measurements demonstrate quantified generation of I atoms during anneals at temperatures below 500 °C when there is TD(N) formation.

The dependency of the concentrations of TD$(N)^+$ centres on anneal time, determined from EPR measurements of p-type Si more lightly doped with B, Al or Ga acceptors, is therefore clarified (figure 15). Initially, as [ΣTD(N)] increases, [ΣTD(N)]$^+$ is expected to increase

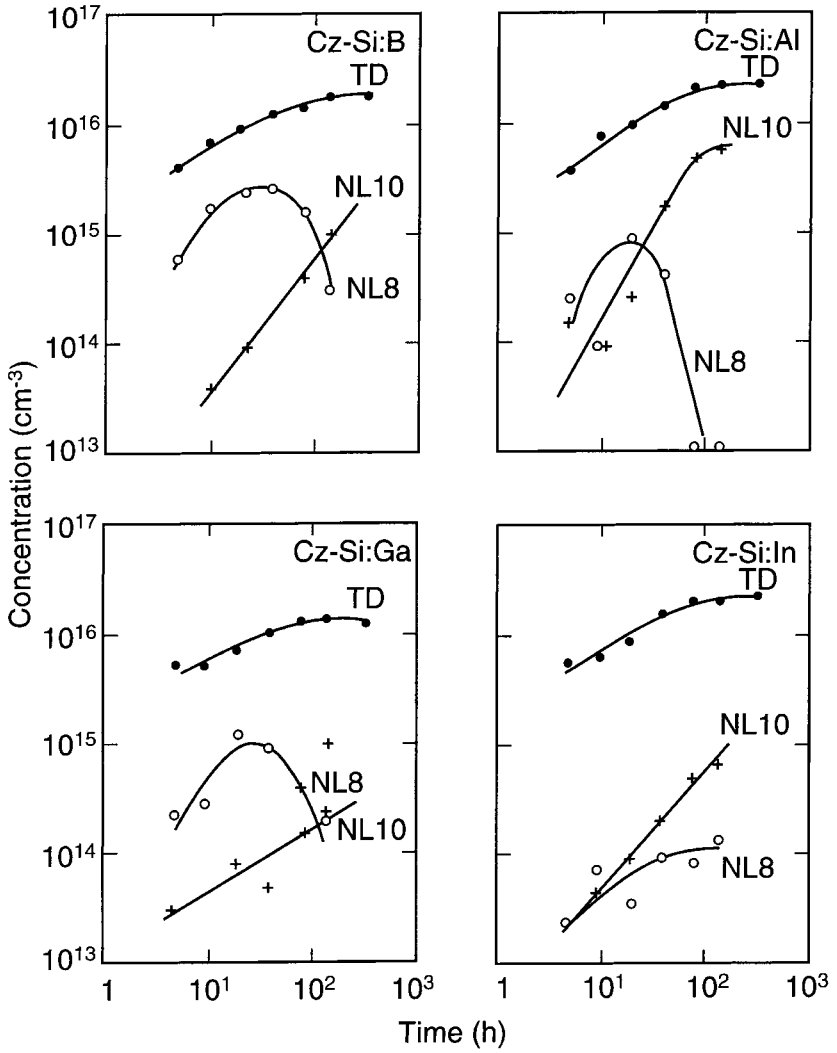

Figure 15. The total concentrations of (a) TD(N) centres determined from resistivity measurements, (b) the associated NL8 EPR spectrum (TD(N)$^+$) and (c) the NL10 EPR spectrum (STD(N)) as a function of anneal time for CZ Si crystals doped with B, Al, Ga or In acceptors. There are progressive reductions in the strengths of the NL8 spectra at extended times for B-, Al- and Ga-doped Si, implying a progressive loss of these acceptors that are expected to exchange sites with I atoms. This reaction does not occur with In acceptors that have a large covalent radius [157].

until it reaches a constant value, equal to the grown-in acceptor concentration. However, after anneals of only ∼20–30 h, the concentration $[\Sigma\mathrm{TD}(N)]^+$ decreases in samples doped with B, Al or Ga [157], implying a loss of these group III acceptors due to an exchange of sites resulting from the capture of I atoms. These measurements therefore support the view that I atoms are formed. It follows that in undoped Si there is sufficient generation of I atoms to be captured by oxygen clusters to form TD(N) defects (see also section 8.2).

Recent IR investigations have shown that oxygen atoms incorporated in TD(N) centres give rise to weak LVMs in the spectral ranges 975–1015 and 724–748 cm^{-1} [158]. Lines at

975, 988, 999 and 1006 cm^{-1} are assigned to TD(1), TD(2), TD(3) and the sum of all the other TD(N) with $N \geqslant 4$ respectively. The integrated absorption coefficients of these electronic transitions corresponds to the expected absorption of only ∼2.0 oxygen atoms, assuming that the oxygen calibration factor is the same as that of isolated O_i atoms. These atoms must therefore be located in the core region of the TD(N) centres as two shells of O_i atoms are resolved by ENDOR measurements. These measurements have, however, so far failed to demonstrate that successive species of the NL8 (and NL10) centres differ by a known number of incorporated oxygen atoms [159]. It had been suggested previously [160] that there may be only, say, *two* oxygen atoms in the core, as shown in figure 13 (the basic Deák model) [102], and the remaining atoms could be bonded self-interstitials. Perhaps this possibility should not yet be ruled out.

TD(1) and TD(2) donors are of special interest as they are bi-stable and show negative-U behaviour [161]. Until recently, these centres were detected only when they were in the double donor state (labelled A) and gave rise to electronic transitions. The new IR measurements show that the LVMs at 975 cm^{-1} (TD(1)) and 988 cm^{-1} (TD(2)) shift to a common line at 1020 cm^{-1} when they transform to the low energy configuration B [162]. These observations have led to much excitement with the expectation that they will shed further light on the bi-stability problem.

It has also been proposed that these centres are each passivated by a single hydrogen atom when they are in the B state [163]. The mechanism of this process is unclear and it is not known whether or not the A state can be passivated.

Since there is evidence that oxygen dimers start to dissociate at $T > 450\,^{\circ}C$, it was of interest to make comparisons with the dissociation of thermal donors [164]. The rate decreases as N increases, as expected (figure 16), because of the increasing sizes of the centres and it was presumed that TD(N) would be transformed into TD($N-1$). However, the rate of decay of TD(1) is much smaller than that of TD(2), implying stronger local bonding at the core, that is not understood.

8.2. STD(N) centres

The STD(N) centres are single donors that also form in CZ Si annealed at temperatures below 500 °C. They give rise to sharp electronic IR absorption lines in the spectral range 150–300 cm^{-1}, that can be detected by IR photo-thermal ionization or absorption spectroscopy (see [165] for a summary of the available data) and an EPR spectrum, labelled NL10. The g-values of this resonance show that the centres are less anisotropic than TD(N) centres, indicating that the unpaired electron is more delocalized [139], consistent with the smaller ionization energies, E_i, derived from the IR data [23]. ^{17}O atoms (in Si enriched with this isotope) detected by ENDOR are assigned to locations in the first two or three atomic shells around the defect core and ^{29}Si ENDOR reveals structure similar to that determined for NL8 centres. The latter measurements also show that the symmetries of adjacent STD(N) donors alternate between C_{2v} and C_s [139], although the IR measurements show only monotonic decreases in E_i with increasing N, with an absence of a staircase structure [23]. Nevertheless, the TD(N) and STD(N) centres must have similar overall structures except that they are double and single donors respectively, implying a difference in the core structure.

There had been a long-standing problem of understanding why the 'same' STD(N) EPR spectrum was found in both Al- and B-doped Si since ENDOR measurements reveal the incorporation of Al, as STDAl(N), donors but not for the formation of corresponding STDB(N), STDGa(N) or STDIn(N) centres. In addition, donors formed in annealed nitrogen doped Si have been ascribed to STDN(N) centres containing a nitrogen atom although ENDOR

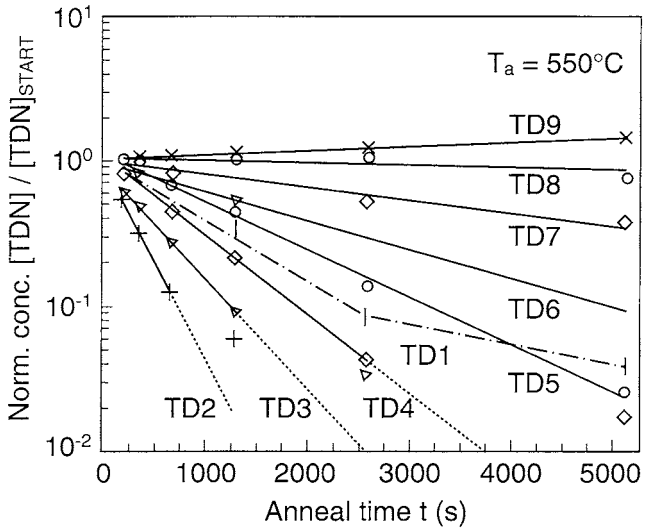

Figure 16. Normalized concentrations $[TD(N)^0]_t/[TD(N)^0]_{START}$ versus anneal time t of rapid transient anneals of a sample containing a high initial concentration of the neutral thermal double donors formed in a prior furnace anneal at 450 °C. The rates of decay of individual donors are indicated by straight lines with slopes that decrease as N increases: the anomalous behaviour of TD(1) implies that this centre is more stable than expected [164].

measurements failed to detect the naturally occurring ^{14}N isotope (see [165] and [23]): likewise STDP(N) centres have not been detected in phosphorus-doped Si [143].

A breakthrough came from high resolution IR measurements made on Si that had been annealed at 1300 °C in hydrogen (or deuterium) gas. Various STD centres were shown to incorporate a hydrogen atom since there were very small reductions in the energies of $\sim$0.1 cm^{-1} of the electronic transitions when incorporated H atoms were replaced by D atoms [23, 137, 166] (figure 17). The shifts, similar to those observed previously for rare-earth–hydrogen pairs, are due to electron–phonon interactions [26, 167]. Hydrogen incorporated in STD centres is also detected by ENDOR in samples that had been pre-heat treated at 1200 °C in water vapour or hydrogen gas [168] and, slightly later, deuterium was also reported [169]. A comparison of the IR and EPR/ENDOR measurements indicated a correlation, as discussed in reference [165], but it is difficult to make a quantitative assessment because of the very different sample requirements for the two techniques.

The IR measurements demonstrated that there were in fact three families of shallow thermal donors [23, 166] (figure 18), with different ionization energies [23]. Two families, namely STDAl(N) and STDH(N), are identified and they can co-exist in samples. Since STDH(N) centres are formed in samples that are *not* deliberately hydrogenated, it follows that hydrogen must be introduced into Si inadvertently during (a) anneals in air or other gases, (b) polishing or (c) growth, as mentioned in section 7.3. The third family of STDX(N) [23, 166] donors has IR frequencies that are the same as those measured by PTIS [170] for samples doped with nitrogen during growth and other samples pre-heated in N_2 gas and annealed at 550 °C. The frequencies are extremely close to those of STDH(N) but the small shifts are real and reproducible. There is no doubt that this is the reason why early IR spectra [171] were attributed to STDN(N). It is also important to note that STDH(N) centres are not stable at 550 °C [23, 166] whereas the concentration of STDX(N) centres increases from that found after anneals at 450 °C. It has been proposed that X may only perturb and stabilize STDH(N) centres since there is no

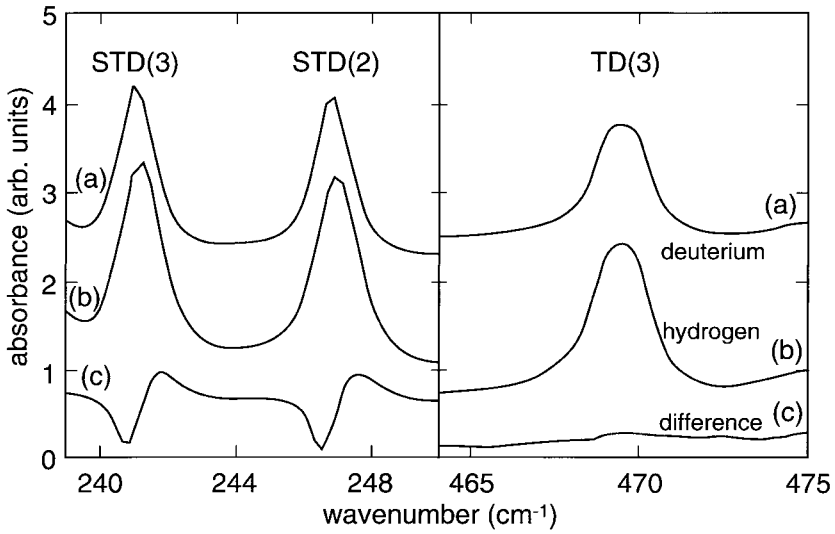

Figure 17. Spectra showing STDH(2) and STDH(3) electronic transitions ($1s \rightarrow 2p_{\pm}$) in samples heated at 470 °C in (a) a deuterium or (b) a hydrogen plasma (13.56 MHz, 40 W, 2 mbar, $t = 70$ h). The transitions in deuterated samples show a frequency shift of $\sim$0.1 cm^{-1} to lower energies compared with hydrogenated samples, as revealed clearly in the difference spectrum (c): these shifts are due to electron–phonon interactions [167]. As expected, there are no corresponding shifts of the frequencies of the TD(N) transitions, since there is no evidence that hydrogen is incorporated in these centres [166].

direct evidence to identify X with a nitrogen atom. Heat treatment of Si in N_2 gas at high temperatures leads to the formation of Si_3N_4 at the surface that leads in turn to the injection of lattice vacancies [172]. The vacancies are mobile and it can be speculated that they are trapped near STDH(N) centres to form STDX(N) donors. It is also significant that the STDH(N) lines correspond to IR lines produced in annealed Si following high energy electron irradiation [173].

A simple explanation can be put forward to explain the formation of STDAl(N) shallow donors on the basis of the Deák model for the structure of TD(N) centres that are predicted to incorporate an I atom [102] generated by the aggregation of oxygen atoms. The I atoms would be captured by substitutional Al atoms that would then be displaced into interstitial sites [146]. There is evidence that Al_i atoms are mobile [150, 174] so that they could then be captured by the two O_i atoms in a TD(N) core (figure 13) and form dative bonds, as for an I atom. The resulting centre would be a single donor, as proposed in earlier work [146], and there would be very strong bonding of Al atoms to oxygen atoms. This is because the heat of formation of Al_2O_3 of $\sim$300 kC mol^{-1} is greater than that of SiO_2 of $\sim$200 kC mol^{-1}: the heats of solution of B_2O_3 and Ga_2O_3 are however only $\sim$200 kC mol^{-1}, similar to that of SiO_2 [175]. It follows that there is a much reduced probability for the formation of STDB(N) and STDGa(N) shallow donors, even though both B_i [115] and Ga_i [150] are mobile.

8.3. The core structure of TD centres

An impression may have been obtained from the discussion presented in sections 8.1 and 8.2 that the problem of determining the core structures of TD(N) and STD(N) centres has been resolved. On the basis of ENDOR measurements, it was assumed that the basic core structure is the same for all the TD centres. The presence of the I atom that can capture a hydrogen atom,

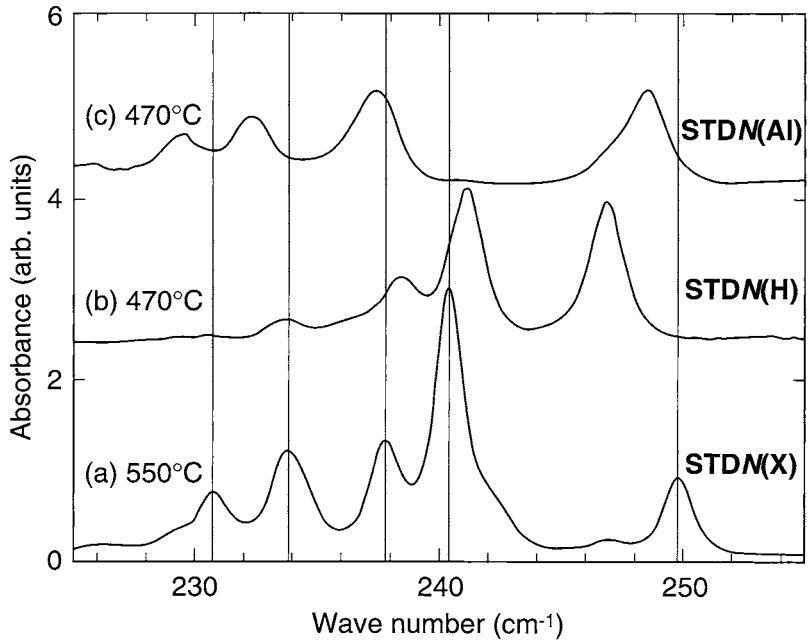

Figure 18. IR absorption lines ($1s \rightarrow 2p_{\pm}$) from (a) Al doped Si, preheated in Ar gas and annealed at 470 °C, showing the STDAl(N) spectrum, (b) hydrogenated Si annealed at 450 °C, showing the STDH(N) spectrum that is not stable at 550 °C and (c) nitrided Si annealed at 550 °C, showing the STDX(N) spectrum. The spectra are all distinct but the small line shifts [23, 163] have led to confusion in identifying these centres in previous work.

or be replaced by an Al atom, to form an STD centre then provides a satisfactory explanation for the growth of these single donors. ENDOR measurements have confirmed that the I–H bond is perpendicular to the plane of the Si–O_i–I–O_i–Si core structure as proposed from theory (figure 13) [102]. However, the hyperfine interactions of H and D atoms do not scale with the moments of the two nuclei [176] and so further refinement of the model is required to obtain agreement with experiment.

9. Conclusions

Many people believe that semiconductor grade monocrystalline silicon is an ultra-pure material that contains only negligible concentrations of impurities and defects. This is true for FZ Si but it often comes as a surprise to learn that CZ Si, used for the fabrication of integrated circuits, contains oxygen at a level of 20 ppma (parts per million atomic). It is also apparent that understanding the diffusion and aggregation of the oxygen atoms in silicon is by no means a simple matter, but the presence of silica precipitates has been considered necessary to getter diffusing metallic contaminants.

Most of the outstanding problems relate to anneals at temperatures below about 700 °C but temperatures in this the range are likely to be required for the fabrication of future integrated circuits because they will have smaller feature sizes. The importance of oxygen was recognized in the earliest period of Si growth; in a second period, it was discovered that the concentration of inadvertently introduced carbon must be less than $\sim 5 \times 10^{15}$ cm^{-3} since the displacement of these impurities into interstitial sites by interactions with I atoms leads to the formation of a

huge number of defects with deep levels [177]; the incorporation of nitrogen was investigated next and found to have certain beneficial effects, but again there is formation of a wide range of complexes; we are now in the 'hydrogen period'. There are problems relating to the control and measurement of hydrogen concentrations and finding reliable methods to identify various complexes. The second part of the review has therefore concentrated on the hydrogen-related issues to give an overview of our current knowledge, although this is not fully comprehensive. However, sufficient references have been given to allow a more complete understanding to be gained.

Acknowledgments

The author thanks R Jones, A R Peaker and J H Tucker (ICSTM) for reading the manuscript and suggesting various changes and T Gregorkiewicz for communicating the information given in [176]. The Physical Science and Engineering Research Council (EPSRC) UK are thanked for their financial support on contract GR/K 96977.

References

[1] Morgan D V and Board K 1983 *An Introduction to Semiconductor Microtechnology* (New York: Wiley)
[2] Pajot B, Artacho E, Ammerlaan C A J and Spaeth J-M 1995 *J. Phys.: Condens. Matter* **7** 7077
[3] Bond W L and Kaiser W 1960 *J. Phys. Chem. Solids* **16** 44
[4] Lederhandler S and Patel J P 1957 *Phys. Rev.* **108** 239
[5] Bullough R, Newman R C, Wakefield J and Willis J B 1960 *J. Appl. Phys.* **31** 707
[6] Sumino K 1994 *Materials, Properties and Preparation Handbook on Semiconductors* vol 3a, ed T S Moss and S Mahajan (Amsterdam: North-Holland) p 73
[7] Hieslmair H, Istratov A A, McHugo S A, Flink C and Weber E 1998 *Semiconductor Silicon 1998: Proc. 8th Int. Symp. on Silicon Materials Science and Technology* vol 98-1, ed H R Huff, U Gösele and H Tsuya (Pennington, NJ: Electrochem. Soc.) p 1127
[8] Takahashi H, Yamada-Kaneta H and Suezawa M 1998 *Japan. J. Appl. Phys.* **37** 1689
[9] Newman R C 1982 *Rep. Prog. Phys.* **45** 1163
[10] Weber E and Gilles D 1990 *Semiconductor Silicon 1990: Proc. 6th Int. Symp. on Silicon Materials Science and Technology* vol 90-7, ed H R Huff, K G Barraclough and J Chikawa (Pennington, NJ: Electrochem. Society) p 585
[11] Newman R C 1992 *Materials Modelling: From Theory to Technology* ed C A English, J R Matthews, H Rauh, A M Stoneham and R Thetford (Bristol: Institute of Physics) p 209
[12] Mikkelsen Jr J C 1986 *Mater. Res. Soc. Symp. Proc.* vol 59 (Pittsburgh, PA: Materials Research Society) p 19
[13] Newman R C and Jones R 1994 *Diffusion of Oxygen in Silicon (Semiconductors and Semimetals 42)* ed F Shimura (San Diego, CA: Academic) pp 289–352
[14] Bullough R and Newman R C 1970 *Rep. Prog. Phys.* **33** 101
[15] Gösele U 1986 *Mater. Res. Soc. Symp. Proc.* vol 59 (Pittsburgh, PA: Materials Research Society) p 419
[16] Gupta A, Messoloras S, Schneider J R, Stewart R J and Zulehner W 1992 *Semicond. Sci. Technol.* **7** 6
[17] Gupta A, Messoloras S, Schneider J R, Stewart R J and Zulehner W 1991 *J. Appl. Crystallogr.* **24** 576
[18] Shimura F and Hockett R S 1986 *Appl. Phys. Lett.* **48** 224
[19] Suezawa M, Sumino K, Harada H and Abe T 1988 *Japan. J. Appl. Phys.* **27** 62
[20] Newman R C 1985 *J. Phys. C: Solid State Phys.* **18** L967
[21] Wagner P and Hage J 1989 *Appl. Phys.* A **49** 123
[22] Götz W, Pensl G and Zulehner W 1992 *Phys. Rev.* B **46** 4312
[23] Newman R C, Ashwin M J, Pritchard R E and Tucker J H 1998 *Phys. Status Solidi* **210** 519
[24] Kaiser W, Frisch H L and Reiss H 1958 *Phys. Rev.* **112** 1546
[25] Hrostowski H and Kaiser R H 1957 *Phys. Rev.* **107** 966
[26] Newman R C 1973 *Infra-Red Studies of Crystal Defects* (London: Taylor and Francis) pp 1–187
[27] Leigh R S and Newman R C 1988 *Semicond. Sci. Technol.* **3** 84
[28] Pajot B and Deltour J P 1967 *Infra-Red Phys.* **7** 195
[29] Bosomworth D R, Hayes W, Spray A R L and Watkins G D 1970 *Proc. R. Soc.* A **317** 133
[30] Artacho E, Ynduráin B, Pajot B, Ramírez R, Herrero C P, Khirunenko L I, Itoh K H and Haller E E 1997 *Phys. Rev.* B **56** 3820
[31] Yamada-Kaneta H 1998 *Phys. Rev.* B **58** 7002

[32] Hallberg T, Murin L I, Lindström J L and Markevitch V P 1998 *J. Appl. Phys.* **84** 2466
[33] Murray R, Graff K, Pajot B, Streijckmans K, Vandendriessche S, Griepink B and Marchandise H 1993 *J. Electrochem. Soc.* **139** 3582
[34] Baghdadi A, Bullis W M, Croarkin M C, Li Y Z, Scace R I, Series R W, Stallhofer P and Watanabe M 1989 *J. Electrochem. Soc.* **136** 2015
[35] Livingston F M, Messoloras S, Newman R C, Pike B C, Stewart R J, Binns M J, Brown W P and Wilkes J G 1984 *J. Phys. C: Solid State Phys.* **17** 6253
[36] Freeland P E 1980 *J. Electrochem. Soc.* **127** 754
[37] Newman R C, Oates A S and Livingston F M 1983 *J. Phys. C: Solid State Phys.* **16** L667
[38] Stavola M 1984 *Appl. Phys. Lett.* **44** 514
[39] Jones R, Öberg S and Umerski A 1992 *Phys. Rev.* B **45** 11321
[40] Southgate P D 1957 *Proc. Phys. Soc.* **70** 804
[41] Southgate P D 1960 *Proc. Phys. Soc.* **36** 385
[42] Haas C 1960 *J. Phys. Chem. Solids* **15** 108
[43] Berry B S and Nowick A S 1966 *Physical Acoustics* vol IIIA, ed W P Mason (New York: Academic) p 1
[44] Corbett J W and Watkins G D 1961 *Phys. Rev. Lett.* **7** 314
[45] Corbett J W, McDonald R C and Watkins G D 1964 *J. Phys. Chem. Solids* **25** 873
[46] Stavola M, Patel J R, Kimerling L C and Freeland P E 1983 *Appl. Phys. Lett.* **42** 73
[47] Newman R C, Tucker J H and Livingston F M 1983 *J. Phys. C: Solid State Phys.* **16** L151
[48] Mikkelsen J C Jr 1982 *Appl. Phys. Lett.* **40** 336
[49] Mikkelsen J C Jr 1982 *Appl. Phys. Lett.* **41** 873
[50] Lee S-T and Nichols D 1985 *Appl. Phys. Lett.* **47** 1001
[51] Lee S-T and Nichols D 1986 *Mater. Res. Soc. Symp. Proc.* vol 59 (Pittsburgh, PA: Materials Research Society) p 31
[52] Messoloras S, Newman R C, Stewart R J and Tucker J H 1987 *Semicond. Sci. Technol.* **2** 4
[53] McQuaid S A, Johnson B K, Gambaro D, Falster R, Ashwin M J and Tucker J H 1999 *J. Appl. Phys.* **86** 1878
[54] Shimura F, Baiardo J P and Fraundorf P 1985 *Appl. Phys. Lett.* **46** 941
[55] Shimura F, Higuchi T and Hockett R S 1988 *Appl. Phys. Lett.* **53** 69
[56] Newman R C and Bean A R 1971 *Radiat. Effects* **8** 189
[57] Davies G, Oates A S, Newman R C, Woolley R, Lightowlers E C, Binns M J and Wilkes J G 1986 *J. Phys. C: Solid State Phys.* **19** 403
[58] Shimura F 1986 *J. Appl. Phys.* **59** 3251
[59] Ham F S 1958 *J. Phys. Chem. Solids* **6** 335
[60] Patrick W, Hearn E, Westdorp W and Bohg A 1979 *J. Appl. Phys.* **50** 7156
[61] Wada K, Inoue N and Kohra K 1980 *J. Crystal Growth* **49** 749
[62] Wada K, Nakanishi J, Takaoka T and Inoue N 1982 *J. Crystal Growth* **57** 337
[63] Bergholz W, Binns M J, Booker G R, Hutchison J C, Kinder S H, Messoloras S, Newman R C, Stewart R J and Wilkes J G 1989 *Phil. Mag.* **59** 499
[64] Taylor W J, Tan T Y and Gösele U 1991 *Proc. 2nd Symp. on Defects in Silicon II* ed W M Bullis, U M Gösele and F Shimura (Pennington, NJ: Electrochem. Society) p 255
[65] Tan T Y, Gardner E E and Tice W K 1977 *Appl. Phys. Lett.* **30** 175
[66] Newman R C 1991 *Proc. 2nd Symp. on Defects in Silicon II* ed W M Bullis, U M Gösele and F Shimura (Pennington, NJ: Electrochem. Society) p 217
[67] Lee S-T, Fellinger P and Chen S 1988 *J. Appl. Phys.* **63** 1924
[68] Lee S-T and Fellinger P 1986 *Appl. Phys. Lett.* **49** 1793
[69] Ourmazd A, Schröter and Bourret A 1984 *J. Appl. Phys.* **56** 1670
[70] Markevich V P, Makarenko L F and Murin L I 1986 *Phys. Status Solidi* a **97** K173
[71] Bourret A 1986 *Mater. Res. Soc. Symp. Proc.* vol 59 (Pittsburgh, PA: Materials Research Society) p 223
[72] Bergholz W, Hutchison J L and Pirouz P 1985 *J. Appl. Phys.* **58** 3419
[73] Bourret A 1987 *Microscopy of Semiconducting Materials (Inst. Phys. Conf. Ser. 87)* ed A G Cullis and P D Augustus (Bristol: Institute of Physics) p 39
[74] Werner P, Reiche M and Hydenreich J 1993 *Phys. Status Solidi* a **137** 533
[75] Takeda S, Kohyama M and Ibe K 1994 *Phil. Mag.* A **70** 287
[76] Stewart R J, Messoloras S and Rycroft S 1996 *Early Stages of Oxygen Precipitation in Silicon (NATO ASI Series 17)* ed R Jones (Dordrecht: Kluwer) p 381
[77] Bender H and Vanhellemont J 1994 *Materials, Properties and Preparation Handbook on Semiconductors* vol 3a, ed T S Moss and S Mahajan (Amsterdam: North Holland) p 1637
[78] Kürner W, Sauer R, Dörnen A and Thonke K 1989 *Phys. Rev.* B **39** 13
[79] Pagani M, Falster R J, Fisher G R, Ferrero G C and Olmo M 1997 *J. Appl. Phys.* **70** 1572

[80] McQuaid S A, Binns M J, Londos C A, Tucker J H, Brown A R and Newman R C 1995 *J. Appl. Phys.* **77** 1427
[81] Tan T Y 1986 *Mater. Res. Soc. Symp. Proc.* vol 59 (Pittsburgh, PA: Materials Research Society) p 195
[82] Gösele U and Tan T Y 1982 *Appl. Phys.* A **28** 79
[83] Gösele U, Ahn K-Y, Marionton B P R, Tan T Y and Lee S-T 1989 *Appl. Phys.* A **48** 219
[84] McQuaid S A, Newman R C and Muñoz E 1995 *Mater. Sci. Forum* **196–201** 1309
[85] Murin L I and Markevich V P 1996 *Early Stages of Oxygen Precipitation in Silicon* ed R Jones (Dordrecht: Kluwer) p 329
[86] Stein H J and Medernach J 1996 *J. Appl. Phys.* **79** 2337
[87] Murin L I, Hallberg T, Markevitch V P and Lindström J L 1998 *Phys. Rev. Lett.* **80** 93
[88] Öberg S, Ewels C P, Jones R, Hallberg T, Lindström J L, Murin L I and Briddon P B 1998 *Phys. Rev. Lett.* **81** 2930
[89] Snyder L C, Corbett J W, Deák P and Wu R 1988 *Mater. Res. Soc. Symp. Proc.* vol 104 (Pittsburgh, PA: Materials Research Society) p 179
[90] Needels M, Joannopoulos J D, Bar-Yam Y and Pantelides S T 1991 *Phys. Rev.* B **43** 4208
[91] Chadi D J 1996 *Phys. Rev. Lett.* **77** 861
[92] Ewels C P, Jones R and Öberg S 1996 *Early Stages of Oxygen Precipitation in Silicon (Nato ASI Series 17)* ed R Jones (Dordrecht: Kluwer) p 141
[93] Claybourn M and Newman R C 1988 *Appl. Phys. Lett.* **52** 2139
[94] Wagner P, Hage J, Trombetta J M and Watkins G D 1992 *Mater. Sci. Forum* **83–87** 401
[95] Watkins G D 1996 *Early Stages of Oxygen Precipitation in Silicon* ed R Jones (Dordrecht: Kluwer) p 1
[96] Watkins G D and Corbett J W 1961 *Phys. Rev.* **121** 1001
[97] Corbett J W, Watkins G D, Chrenko R M and McDonald R S 1961 *Phys. Rev.* **121** 1015
[98] Bean A R and Newman R C 1971 *Solid State Commun.* **9** 271
[99] Oates A S and Newman R C 1986 *Appl. Phys. Lett.* **49** 262
[100] Brelot A and Charlemagne J 1971 *Radiation Effects in Semiconductors* ed J W Corbett and G D Watkins (London: Gordon and Breach) p 161
[101] Abdullin Kh A, Mukashev B N and Gorelkinski Yu V 1995 *Mater. Sci. Forum* **196–201** 1007
[102] Deák P, Snyder L C and Corbett J W 1992 *Phys. Rev.* B **45** 11 612
[103] Brelot A 1972 *PhD Thesis* University of Paris
[104] Davies G Lightowlers E C, Newman R C and Oates A S 1987 *Semicond. Sci. Technol.* **2** 524
[105] Newman R C, Oates A S and Livingston F M 1983 *J. Phys. C: Solid State Phys.* **16** L667
[106] Oates A S, Binns M J, Newman R C, Tucker J H, Wilkes J G and Wilkinson A 1984 *J. Phys. C: Solid State Phys.* **17** 5695
[107] Brelot A 1973 *Radiation Damage and Defects in Semiconductors (Inst. Phys. Conf. Ser. 16)* ed J E Whitehouse (Bristol: Institute of Physics) p 191
[108] Watkins G D 1975 *Phys. Rev.* B **12** 4383
[109] Oates A S, Newman R C and Tucker J H 1985 *13th Int. Conf. on Defects in Semiconductors* ed L C Kimerling and J M Parsey Jr (New York: AIME) p 709
[110] Newman R C, Tipping A K and Tucker J H 1986 unpublished
[111] Svensson B G and Lindström J L 1986 *Phys. Rev.* B **34** 8709
[112] Awadelkarim O O, Weman H, Svensson B G and Lindström J L 1986 *J. Appl. Phys.* **60** 1974
[113] Istratov A A, Hedemann H, Seibt M, Vyvenko O F, Schröter W, Flink C, Heiser T, Hieslmair H and Weber E R 1998 *Proc. 8th Int. Symp. on Silicon Materials Science and Technology 98-1* ed H R Huff, T Tsuya and U Gošele (Pennington, NJ: Electrochem. Society) p 948
[114] Newman R C, Tipping A K and Tucker J H 1985 *J. Phys. C: Solid State Phys.* **18** L861
[115] Tipping A K and Newman R C 1987 *Semicond. Sci. Technol.* **2** 315
[116] Hanson W L, Haller E E and Luke P N 1982 *IEEE Trans. Nucl. Sci.* **29** 738
[117] Fuller C S and Logan R A 1957 *J. Appl. Phys.* **28** 1427
[118] Stavola M, Patel J R, Kimerling L C and Freeland P E 1983 *Appl. Phys. Lett.* **42** 73
[119] Brown A R, Claybourn M, Murray R, Nandhra P S, Newman R C and Tucker J H 1988 *Semicond. Sci. Technol.* **3** 591
[120] Newman R C, Tucker J H, Brown A R and McQuaid S A 1991 *J. Appl. Phys.* **70** 3061
[121] Binns M J, McQuaid S A, Newman R C and Lightowlers E C 1993 *Semicond. Sci. Technol.* **8** 1908
[122] Newman R C, Pritchard R E, Tucker J H and Lightowlers E C 1999 *Phys. Rev.* B **60** 12 775
[123] Van Wieringen A and Warmoltz W 1956 *Physica* **22** 849
[124] Pritchard R E, Ashwin M J, Tucker J H, Newman R C, Lightowlers E C, Binns M J, McQuaid S A and Falster R 1997 *Phys. Rev.* B **56** 13 118
[125] Pritchard R E, Ashwin M J, Tucker J H and Newman R C 1998 *Phys. Rev.* B **57** 15 048
[126] Hourahine B, Jones R, Öberg S, Newman R C, Briddon P R and Roduner E 1998 *Phys. Rev.* B **57** 12 666

[127] Murakami K, Fukata N, Sasaki S, Ishioka K, Kiyajima M, Fujimura S, Kikuchi J and Haneda H 1996 *Phys. Rev. Lett.* **77** 3161
[128] Leitch A W R, Alex V and Weber J 1998 *Phys. Rev. Lett.* **81** 421
[129] Estreicher S K 1990 *Phys. Rev.* B **41** 9886
[130] Jones R, Öberg S and Umerski A 1991 *Mater. Sci. Forum* **83–87** 551
[131] Ramamoorthy M and Pantelides S T 1996 *Phys. Rev. Lett.* **76** 267
[132] Capaz R B, Assali L V C, Kimerling L C, Cho K and Joannopoulos J D 1999 *Phys. Rev.* B **59** 4898
[133] Bech-Nielsen B, Tanderup K, Budde M, Bonde-Nielsen K, Lindström J L, Jones R, Öberg S, Hourahine B and Briddon P 1997 *Mater. Sci. Forum* **258–263** 391
[134] Van de Walle C G 1994 *Phys. Rev.* B **49** 4579
[135] Maddalon-Vinante C, Barbier D, Erramli H and Blondiaux G 1993 *J. Appl. Phys.* **74** 6115
[136] Tokuda Y, Katoh I, Ohshima H and Hattori T 1994 *Semicond. Sci. Technol.* **9** 1733
[137] McQuaid S A, Newman R C and Lightowlers E C 1994 *Semicond. Sci. Technol.* **9** 1736
[138] Lee K M, Trombetta J M and Watkins G D 1986 *Mater. Res. Soc. Symp. Proc.* vol 46 (Pittsburgh, PA: Materials Research Society) p 263
[139] Gregorkiewicz T, Bekman H H P Th and Ammerlaan C A J 1988 *Phys. Rev.* B **38** 3998
[140] Dirksen R, Berg-Rasmussen F, Gregorkiewicz T and Ammerlaan C A J 1997 *Mater. Sci. Forum* **258–263** 373
[141] Dirksen R, Gregorkiewicz T and Ammerlaan C A J 1998 *Phys. Status Solidi* **210** 539
[142] Michel J, Nicklas J R and Spaeth J-M 1989 *Phys. Rev.* B **40** 1732
[143] Spaeth J-M 1996 *Early Stages of Oxygen Precipitation in Silicon* vol 17, ed R Jones (Dordrecht: Kluwer) p 83
[144] Chadi J 1996 *Phys. Rev. Lett.* **77** 861
[145] Bean A R and Newman R C 1972 *J. Phys. Chem. Solids* **33** 255
[146] Newman R C 1990 *20th Int Conf on the Physics of Semiconductors* vol 1, ed E M Anastassakis and J D Joannopoulis (Singapore: World Scientific) p 525
[147] Newman R C and Bean A R 1971 *Radiat. Effects* **8** 189
[148] Lightowlers E C, Newman R C and Tucker J H 1994 *Semicond. Sci. Technol.* **9** 1370
[149] Safanov A N, Lightowlers E C, Davies G, Leary P, Jones R and Öberg S 1996 *Phys. Rev. Lett.* **77** 4812
[150] Watkins G D 1965 *Radiation Effects in Semiconductors* (Paris: Dunod) p 97
[151] Windl W, Bunea M M, Strumpf R, Dunham S T and Masquelier M P 1999 *Phys. Rev. Lett.* **83** 4345
[152] Sadigh B, Lenosky T J, Theiss S K, Caturla M-J, Rubia T D and Foad M A 1999 *Phys. Rev. Lett.* **83** 4341
[153] Tipping A K and Newman R C 1987 *Semicond. Sci. Technol.* **2** 389
[154] Newman R C 1981 *Neutron Transmutation Doped Silicon* ed J Guldberg (New York: Plenum) p 83
[155] Claybourn M and Newman R C 1989 *Mater. Sci. Forum* **38–41** 613
[156] Fuller C S, Doleiden F H and Wolfstern K B 1960 *J. Phys. Chem. Solids* **13** 187
[157] Gregorkiewicz T, van Wezep D A, Bekman H H P Th and Ammerlaan C A J 1987 *Phys. Rev.* B **35** 3870
[158] Hallberg T and Lindström J L 1996 *J. Appl. Phys.* **79** 7570
[159] Ammerlaan C A J, Zevenbergen I S, Martynov Yu V and Gregorkievicz T 1996 *Early Stages of Oxygen Precipitation in Silicon* vol 17, ed R Jones (Dordrecht: Kluwer) p 61
[160] Newman R C 1986 *Mater. Res. Soc. Symp. Proc.* vol 59 (Pittsburgh, PA: Materials Research Society) p 205
[161] Tkachev V D, Makarenko L F, Markevich V P and Murin L I 1984 *Sov. Phys.–Semicond.* **18** 324
[162] Hallberg T and Lindström J L 1996 *Appl. Phys. Lett.* **68** 3458
[163] Bohne D I and Weber J 1993 *Phys. Rev.* B **47** 4037
[164] Götz W, Pensl G, Zulener W, Newman R C and McQuaid S A 1998 *J. Appl. Phys.* **84** 3561
[165] Newman R C, Tucker J H, Semaltianos N G, Lightowlers E C, Gregorkiewicz T, Zevenbergen I S and Ammerlaan C A J 1996 *Phys. Rev.* B **54** R6803
[166] Pritchard R E, Ashwin M J, Tucker J H, Newman R C, Lightowlers E C, Gregorkiewicz T, Zevenbergen I S, Ammerlaan C A J, Falster R and Binns M J 1997 *Semicond. Sci. Technol.* **12** 1404
[167] Newman R C 1969 *Adv. Phys.* **18** 545
[168] Martynov Yu, Gregorkiewicz T and Ammerlaan C A J 1995 *Phys. Rev. Lett.* **74** 2030
[169] Martynov Yu, Gregorkiewicz T and Ammerlaan C A J 1995 *Mater. Sci. Forum* **196–201** 849
[170] Griffin J, Hartung J, Weber J, Navarro H and Genzel L 1989 *Appl. Phys.* A **48** 41
[171] Hara A 1995 *Japan. J. Appl. Phys.* **34** 3418
[172] Fahy P M, Griffin P B and Plummer J D 1989 *Rev. Mod. Phys.* **61** 289
[173] Markevich V P, Suezawa M, Sumino K and Murin L I 1994 *J. Appl. Phys.* **76** 7347
[174] Devine S D and Newman R C 1970 *J. Phys. Chem. Solids* **31** 685
[175] Bullough R, Newman R and Wakefield J 1959 *Proc. IEE* B **106** (Supplement 15) 277
[176] Martynov Yu V 1996 *PhD Thesis* University of Amsterdam
[177] Davies G and Newman R C 1994 *Handbook on Semiconductors* 2nd edn, vol 3(b), ed S Mahajan (Amsterdam: North-Holland) p 1557